

AD-A273 263

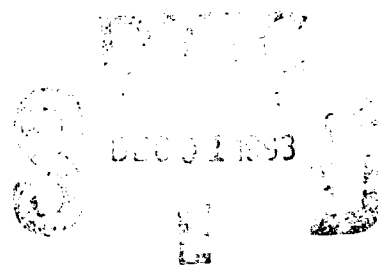


2

NAVAL POSTGRADUATE SCHOOL Monterey, California



THESIS



Free-Surface/Vorticity Interaction

by

John B. Carroll

September 1993

Thesis Advisor:

T. Sarpkaya

Approval for public release; distribution is unlimited.

93-29342



5788

93 11 30 042

Unclassified

SECURITY CLASSIFICATION OF THIS PAGE

REPORT DOCUMENTATION PAGE				Form Approved OMB No. 0704-0188	
1a. REPORT SECURITY CLASSIFICATION Unclassified			1b. RESTRICTIVE MARKINGS		
2a. SECURITY CLASSIFICATION AUTHORITY			3. DISTRIBUTION AVAILABILITY OF REPORT		
2b. DECLASSIFICATION/DOWNGRADING SCHEDULE			Approved for public release; distribution unlimited.		
4. PERFORMING ORGANIZATION REPORT NUMBER(S)			5. MONITORING ORGANIZATION REPORT NUMBER(S)		
6a. NAME OF PERFORMING ORGANIZATION Naval Postgraduate School		6b OFFICE SYMBOL (If applicable) ME	7a. NAME OF MONITORING ORGANIZATION Naval Postgraduate School		
6c. Address (City, State, and ZIP Code) Monterey, CA 93943-5000			7b. ADDRESS (City, State, and ZIP Code) Monterey, CA 93943-5000		
8a. NAME OF FUNDING/SPONSORING ORGANIZATION		8b OFFICE SYMBOL (If applicable)	9. PROCUREMENT INSTRUMENT IDENTIFICATION NUMBER		
8c. ADDRESS (City, State, and ZIP Code)			10. SOURCE OF FUNDING NUMBERS		
			PROGRAM ELEMENT No.	PROJECT No.	TASK No.
			WORK UNIT ACCESSION No.		
11. TITLE (Include Security Classification) Free-Surface/Vorticity Interaction					
12. PERSONAL AUTHOR(S) JOHN B. CARROLL					
13a. TYPE OF REPORT Thesis for Master of Science and Mechanical Engineer Degrees		13b. TIME COVERED From:		14. DATE OF REPORT (Year, Month, Day) 1993 September	
				15. PAGE COUNT 57	
16. SUPPLEMENTARY NOTATION The views expressed in this thesis are those of the author and do not reflect the official policy or position of the Department of Defense or the U. S. Government.					
17. COSATI CODES			18. SUBJECT TERMS (Continue on reverse if necessary and identify by block number)		
FIELD	GROUP	SUB-GROUP	Surface Disturbances, Scars, Striations, Trailing Vortices, Vortex Dynamics		
19. ABSTRACT (Continue on reverse if necessary and identify by block number)					
<p>The unsteady flow phenomena resulting from the interaction of wakes and vortices with the free surface are of particular importance in naval hydrodynamics. Ship and submarine wakes produce a three-dimensional complex signature, comprised of a narrow dark band bordered by two bright lines in synthetic-aperture-radar (SAR) images. The dark band signifies the suppression of waves at the Bragg frequency as a consequence of the interaction between the free surface and the imposed vorticity. In the present investigation, the vorticity field is provided by a single tip vortex generated by an airfoil. The results, obtained with an LDV, have shown that the free surface redistributes part or all of the normal turbulent kinetic energy into streamwise and spanwise components. The turbulent kinetic energy first decreases sharply with increasing vertical distance from the vortex and then remains nearly constant within a thin layer below the 'roughened' free surface. The results explain the longevity of the structures and lend further credence to the simulation of near-surface structures via vortex- or contour-dynamics.</p>					
20. DISTRIBUTION/AVAILABILITY OF ABSTRACT (x) unclassified/unlimited () same as RPT () DTIC users			21. ABSTRACT SECURITY CLASSIFICATION Unclassified		
22a. NAME OF RESPONSIBLE INDIVIDUAL Professor T. Sarpkaya			22b TELEPHONE (Include Area code) (408) 656-3425		22c. OFFICE SYMBOL ME-SL

DD Form 1473, JUN 86

Previous editions are obsolete.

SECURITY CLASSIFICATION OF THIS PAGE

Unclassified

Approved for public release; distribution is unlimited.

Free-Surface/Vorticity Interaction

by

John B. Carroll
Lieutenant, United States Navy
B.S.M.E., Worcester Polytechnic Institute, 1984

Submitted in partial fulfillment of the
requirements for the degree of

MASTER OF SCIENCE IN MECHANICAL ENGINEERING

AND

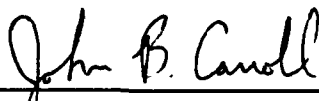
MECHANICAL ENGINEER

from the

NAVAL POSTGRADUATE SCHOOL

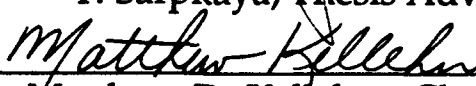
September 1993

Author:


John B. Carroll

Approved by:


T. Sarpkaya, Thesis Advisor


Matthew D. Kelleher, Chairman,
Department of Mechanical Engineering


Richard S. Elster, Dean of Instruction

ABSTRACT

The unsteady flow phenomena resulting from the interaction of wakes and vortices with the free surface are of particular importance in naval hydrodynamics. Ship and submarine wakes produce a three-dimensional complex signature, comprised of a narrow dark band bordered by two bright lines in synthetic-aperture-radar (SAR) images. The dark band signifies the suppression of waves at the Bragg frequency as a consequence of the interaction between the free surface and the imposed vorticity. In the present investigation, the vorticity field is provided by a single tip vortex generated by an airfoil. The results, obtained with an LDV, have shown that the free surface redistributes part or all of the normal turbulent kinetic energy into streamwise and spanwise components. The turbulent kinetic energy first decreases sharply with increasing vertical distance from the vortex and then remains nearly constant within a thin layer below the 'roughened' free surface. The results explain the longevity of the structures and lend further credence to the simulation of near-surface structures via vortex- or contour-dynamics.

Accession For	
NTIS CRA&I	<input checked="" type="checkbox"/>
DTIC TAB	<input type="checkbox"/>
Unannounced	<input type="checkbox"/>
Justification	
By	
Distribution /	
Availability Codes	
Dist	Availability Codes
A-1	

TABLE OF CONTENTS

I. INTRODUCTION.....	1
II. EXPERIMENTAL EQUIPMENT.....	4
III. DISCUSSION OF RESULTS	6
A. DISCUSSION OF VELOCITIES	6
B. DISCUSSION OF TURBULENCE MEASUREMENTS	7
IV. CONCLUSIONS	13
APPENDIX.....	14
REFERENCES.....	46
INITIAL DISTRIBUTION LIST.....	48

LIST OF FIGURES

Figure 1.	Definition Sketch	14
Figure 2.	U/U_o versus Lateral Distance for $Z/h_o = 0.58$ and $x/c = 5.02$	15
Figure 3.	U/U_o versus Lateral Distance for $Z/h_o = 0.00$ and $x/c = 5.02$	16
Figure 4.	U/U_o versus Vertical Distance for $Y/h_o = -0.27$ and $x/c = 5.02$	17
Figure 5.	U/U_o versus Vertical Distance for $Y/h_o = 0.00$ and $x/c = 5.02$	18
Figure 6.	W/U_o versus Lateral Distance for $Z/h_o = 0.38$ and $x/c = 5.02$	19
Figure 7.	W/U_o versus Lateral Distance for $Z/h_o = 0.00$ and $x/c = 5.02$	20
Figure 8.	W/U_o versus Vertical Distance for $Y/h_o = -0.40$ and $x/c = 5.02$	21
Figure 9.	W/U_o versus Vertical Distance for $Y/h_o = -0.27$ and $x/c = 5.02$	22
Figure 10.	V/U_o versus Vertical Distance for $Y/h_o = 0.00$ and $x/c = 5.02$	23
Figure 11.	U/U_o versus Lateral Distance for $Z/h_o = 0.85$ and $x/c = 6.52$	24
Figure 12.	U/U_o versus Lateral Distance for $Z/h_o = 0.00$ and $x/c = 6.52$	25
Figure 13.	U/U_o versus Vertical Distance for $Y/h_o = -0.46$ and $x/c = 6.52$	26
Figure 14.	U/U_o versus Vertical Distance for $Y/h_o = 0.25$ and $x/c = 6.52$	27
Figure 15.	U/U_o versus Vertical Distance for $Y/h_o = 0.65$ and $x/c = 6.52$	28
Figure 16.	W/U_o versus Lateral Distance for $Z/h_o = 0.85$ and $x/c = 6.52$	29
Figure 17.	W/U_o versus Lateral Distance for $Z/h_o = 0.62$ and $x/c = 6.52$	30
Figure 18.	W/U_o versus Lateral Distance for $Z/h_o = 0.00$ and $x/c = 6.52$	31
Figure 19.	W/U_o versus Vertical Distance for $Y/h_o = -0.44$ and $x/c = 6.52$	32
Figure 20.	W/U_o versus Vertical Distance for $Y/h_o = -0.25$ and $x/c = 6.52$	33
Figure 21.	u'/U_o versus Lateral Distance for $Z/h_o = 0.60$ and $x/c = 5.02$	34
Figure 22.	u'/U_o versus Lateral Distance for $Z/h_o = 0.00$ and $x/c = 5.02$	35
Figure 23.	u'/U_o versus Vertical Distance for $Y/h_o = -0.27$ and $x/c = 5.02$	36

Figure 24.	u'/U_o versus Vertical Distance for $Y/h_o = 0.60$ and $x/c = 5.02$	37
Figure 25.	v'/U_o versus Vertical Distance for $Y/h_o = 0.00$ and $x/c = 5.02$	38
Figure 26.	w'/U_o versus Lateral Distance for $Z/h_o = 0.38$ and $x/c = 5.02$	39
Figure 27.	w'/U_o versus Lateral Distance for $Z/h_o = 0.00$ and $x/c = 5.02$	40
Figure 28.	w'/U_o versus Vertical Distance for $Y/h_o = -0.40$ and $x/c = 5.02$	41
Figure 29.	w'/U_o versus Vertical Distance for $Y/h_o = -0.15$ and $x/c = 5.02$	42
Figure 30.	u'/U_o versus Vertical Distance for $Y/h_o = -0.46$ and $x/c = 6.52$	43
Figure 31.	w'/U_o versus Vertical Distance for $Y/h_o = -0.25$ and $x/c = 6.52$	44
Figure 32.	Normalized Turbulent Kinetic Energy versus Vertical Distance	45

LIST OF SYMBOLS

c	= Chord length of foil
E	= Turbulent kinetic energy
E_{min}	= Minimum turbulent kinetic energy
h_o	= Depth of vortex from free surface
Re	= Reynolds number, $U_o c / \nu$
U	= Axial component of velocity
U_o	= Velocity of ambient flow
u'	= RMS value of u'
V	= Transverse component of velocity
v'	= RMS value of v'
W	= Vertical component of velocity
w'	= RMS value of w'
x	= Axial coordinate, origin at vortex
y	= Lateral coordinate, origin at vortex
z	= Vertical coordinate, origin at vortex
Γ	= Circulation of vortex
ν	= Kinematic viscosity

ACKNOWLEDGMENTS

Thanks are due Mr. Jack McKay for his help in the form of machine shop support and tank set-up.

This thesis is an extension of the work started by LT Donald E. Neubert, Jr. His instruction on the operation and alignment of the laser doppler anemometer system was of great assistance.

The Office of Naval Research is owed thanks for its continued support of the on-going research effort into vortex interactions here at the Naval Postgraduate School.

Finally, and most importantly, this thesis is just a small part of a groundbreaking exploration into vortex dynamics by Distinguished Professor T. Sarpkaya. It is his guidance, scientific expertise, help with the composition of this work and love of fluid mechanics that has made this effort possible.

I. INTRODUCTION

The unsteady flow phenomena resulting from the interaction of wakes and vortices with the free surface are of particular importance in naval hydrodynamics. Ship wakes produce a three-dimensional complex signature, comprised of a narrow dark band bordered by two bright lines in synthetic-aperture-radar (SAR) images. The dark band is the most prominent of all the signatures and is seen many kilometers downstream at all angles to the SAR azimuth direction even under severe weather conditions. It signifies the suppression of waves at the Bragg frequency as a consequence of various short-wave-damping phenomena such as turbulence, surface-active materials, and the redistribution of surface impurities. The two bright lines, on the other hand, each resembling a moonglade, manifest themselves only in light winds and signify the occurrence of a range of waves which happen to be near the Bragg wavelength, possibly as a consequence of the interaction between quasi-two-dimensional turbulent motions near the free surface and the restructuring and modulation of this interaction by wind.

The foregoing strongly suggests that the three-dimensional turbulent flow field beneath the free surface, the extent of the two-dimensionalization of turbulence with depth, and the reverse energy cascade process near the free surface must be understood in as much detail as possible in order to gain some insight into the occurrence of surface signatures. One of the simplest possible flows relevant to the dynamical processes in vorticity/free-surface interaction which can be carefully studied in isolation, without complications and competing influences that normally occur in a fully turbulent ship wake, is the interaction of a single turbulent vortex with the free surface of an otherwise smooth uniform flow. The modulations of the flow field and

turbulence near the free surface are not expected to be similar to that observed for a streamwise vortex in or near a rigid-wall boundary layer (Harvey and Perry, 1971; Shabaka, Melville, and Bradshaw, 1985).

Extensive reviews of the interaction of a pair of heterostrophic vortices with a free surface are given by Sarpkaya (1986, 1992a, 1992b), Sarpkaya, Elnitsky, and Leeker (1988) and Sarpkaya and Suthon (1991), wherein it is suggested that the free surface signatures (scars) exhibit features that obey the decay laws of two-dimensional turbulence. The reverse energy cascade process dominates the turbulence behavior near the free surface through the interaction and merging of homostrophic vortices. The energy and enstrophy inertial ranges coexist, with an upscale energy transfer and downscale enstrophy transfer in the same wavenumber interval. The quasi-two-dimensionalization of turbulence in various types of flows (Jacquin, Leuchter, and Geffroy, 1989; Hunt and Graham, 1978), in general, and near a free surface (Loewen, Ahlborn, and Filuk, 1986; Brumley, 1984; Dickey, Hartman, Hammond, and Hurst, 1984; Komori, Ueda, Ogino, and Mizushima, 1982; Rashidi, and Banerjee, 1988; Lam, and Banerjee, 1992; Anthony, 1992; Komori, Nagaosa, Murakami, Chiba, Ishii, and Kuwahara, 1993), in particular, has emerged as a fundamental phenomenon during the past decade.

In view of the foregoing, an experimental investigation on the flow structure resulting from the interaction of a single tip vortex with a deformable free surface was undertaken (Neubert, 1992; Sarpkaya and Neubert, 1993). The present study is a continuation of this investigation in much greater detail as far as the velocity and turbulence measurements are concerned. The results have shown that the free surface redistributes part or all of the normal turbulent kinetic energy into streamwise and spanwise components. The turbulent kinetic energy first decreases sharply with

increasing vertical distance from the vortex and then remains nearly constant within a thin layer below the 'roughened' free surface. The results lend further credence to the simulation of near-surface structures by a decaying 2-D turbulence through the use of vortex element methods.

II. EXPERIMENTAL EQUIPMENT

The experiments were conducted in a low turbulence water tunnel with an open test section of about 40 cm wide, 50 cm deep (maximum), and 125 cm long. The turbulence management system is located upstream of the test section. It consists of a honeycomb and a fine-mesh screen. The tunnel is driven by a 50 Hp centrifugal pump. A second but smaller pump continuously circulated the tunnel water through a micro filtration system to remove rust and other suspended fine particles, down to about 1 μm , from the water (the filtration system was turned off during the experiments). A skimmer, placed upstream of the turbulence management system and connected to another filter, was operated continuously to maintain the free surface clean.

A 6% thick, rectangular planform, symmetric, Joukowski half-span foil with an effective aspect ratio of 10.4 was used to generate a 'single' trailing vortex. The tip of the foil was carefully rounded. The model foil was mounted in a rotatable cylindrical base, embedded into the bottom of the test-section floor. The angle of attack was varied from 6° to 12° and the water level was held constant. The interior of the model was hollowed and connected to a dye reservoir to seed the vortex core with a fluorescent dye. The leading edge of the foil was 3.6 chord lengths downstream of the test section entrance.

The mean velocities and turbulence intensities were measured with a Laser-Doppler Anemometer. Bragg-cell frequency shifting by 0.5 MHz was used in one channel to detect the flow reversals. The probe volume (approximately 200 μm in diameter) was positioned at the required location by use of a remotely driven x-y-z traversing unit. The scattering particles used

were titanium dioxide of rutile crystalline form and were approximately 12 μm in size. All measurements were made using 1024 point ensembles. The data are reported without any velocity-bias-correction.

A single vortex position relative to the free surface and two measurement stations relative to the trailing edge of the foil were considered. The vortex axis was $h_0 = 25$ mm below the free surface. The velocity and turbulence measurements were made along several $y/h_0 = \text{constant}$ (vertical lines) and $z/h_0 = \text{constant}$ (horizontal lines) at two stations along the vortex (5.0 and 6.5 chord lengths downstream from the trailing edge of the foil). The chord-based Reynolds number was $U_0 c / \nu = 45,000$, ($\Gamma / \nu = 2,500$), and the vortex circulation was about $\Gamma / U_0 c = 0.50$. Here only the most representative results will be discussed in terms of velocities and the RMS values of turbulence, denoted by u' , v' , and w' and normalized by U_0 .

III. DISCUSSION OF RESULTS

A. DISCUSSION OF VELOCITIES

The coordinated axes and velocities are shown in Fig. 1. The axial velocity, normalized by the mean velocity U_0 , is shown in Figs. 2 and 3 for $z/h_0 = 0.58$ and $z/h_0 = 0.0$, respectively, for $x/c = 5.02$. The axial velocity along representative vertical lines is shown in Figs. 4 and 5 as a function of z/h_0 for $y/h_0 = -0.27$ and $y/h_0 = 0.0$, for $x/c = 5.02$. Figures 2-5 show that the presence of the vortex leads to an axial velocity defect directly above the vortex axis. The axial velocity recovers quickly both along the horizontal and vertical lines as the values of either y/h_0 or z/h_0 increase.

The vertical component of velocity, again normalized by U_0 , is shown in Figs. 6 and 7 (for $z/h_0 = 0.38$ and $z/h_0 = 0.0$) and in Figs. 8 and 9 (for $y/h_0 = -0.40$ and $y/h_0 = -0.27$), all for $x/c = 5.02$. It is clear that the magnitude of the vertical component of velocity exhibits the usual vortex behavior near the vortex axis. This is particularly evident along the horizontal lines. Along the z axis, the magnitude of W/U_0 decreases sharply as one approaches the free surface (Figs. 8 and 9). A representative plot of the lateral component of velocity V/U_0 is shown in Fig. 10 for $y/h_0 = 0.0$. It exhibits the usual vortex velocity distribution along a vertical line.

The axial velocity, normalized by the mean velocity U_0 , is shown in Figs. 11 and 12 for $z/h_0 = 0.85$ and $z/h_0 = 0.0$, respectively, for $x/c = 6.52$. The axial velocity along representative vertical lines is shown in Figs. 13 through 15 a function of z/h_0 for $y/h_0 = -0.46$, $y/h_0 = 0.25$, and $y/h_0 = 0.65$, for $x/c = 6.52$. Figures 11-15 show that the presence of the vortex leads to an axial velocity defect at or near the vortex axis. The axial velocity recovers quickly both

along the horizontal and vertical lines as the values of either y/h_0 or z/h_0 increase.

The vertical component of velocity, again normalized by U_0 , is shown in Figs. 16 through 18 (for $z/h_0 = 0.85, 0.62$ and $z/h_0 = 0.0$) and in Figs. 19 and 20 (for $y/h_0 = -0.45$ and $y/h_0 = -0.25$), all for $x/c = 6.52$. Once again, it is clear that the magnitude of the vertical component of velocity exhibits the usual vortex behavior near the vortex axis. This is particularly evident along the horizontal lines. Along the z axis, the magnitude of W/U_0 decreases sharply as one approaches the free surface.

B. DISCUSSION OF TURBULENCE MEASUREMENTS

The turbulence intensity $u'/U_0 = \sqrt{u'^2} / U_0 =$ Root-Mean-Square value of the u' -component of turbulence normalized by U_0 is shown as a function of y/h_0 in Figs. 21 and 22 for $z/h_0 = 0.60$ and $z/h_0 = 0.0$, and in Figs. 24 and 25 for $y/h_0 = -0.27$ and $y/h_0 = 0.0$, all for $x/c = 5.02$. It is clear from the last two figures that u'/U_0 first decreases as z/h_0 increases and then, very near the free surface, it increases sharply. Figure 25 shows v'/U_0 as a function of z/h_0 for $y/h_0 = 0.0$ and $x/c = 5.02$. Once again, v'/U_0 also decreases with increasing z/h_0 as one approaches the free surface. However, very near the free surface v'/U_0 increases sharply, almost doubling its value. On the basis of these observations, an increase in w'/U_0 will require an explanation for the increase in turbulent kinetic energy and a decrease in w'/U_0 will signify the increase of anisotropy and the quasi-two-dimensionalization of an otherwise nearly isotropic turbulence.

Figures 26 and 27 show representative horizontal profiles of w'/U_0 at $z/h_0 = 0.38$ and at $z/h_0 = 0.0$ for $x/c = 5.02$. Figures 28 and 29 show representative profiles of w'/U_0 at $y/h_0 = -0.40$ and at $z/h_0 = -0.15$ for $x/c =$

5.02. Clearly, w'/U_0 decreases with increasing z/h_0 for a given y/h_0 . However, unlike u'/U_0 and v'/U_0 , w'/U_0 does not exhibit an increase near the free surface. This signals an interesting metamorphosis as far as the effect of the free surface on turbulence is concerned. The turbulence becomes much more anisotropic and the reduction in w'/U_0 (the reflection of vertical momentum from the free surface) leads to an increase in u'/U_0 and v'/U_0 . It is, therefore, important to explore the variation of the turbulent kinetic energy, particularly in the region where the two-dimensionalization of turbulence occurs.

Figures 30 and 31 show u'/U_0 and w'/U_0 versus z/h_0 for $y/h_0 = -0.46$ and $y/h_0 = -0.25$, respectively, all for $x/c = 6.52$. Once again, it is clear that while u'/U_0 begins to increase near the free surface, the w'/U_0 component of turbulence continues to decrease. There is no doubt that v'/U_0 exhibits a similar behavior at $x/c = 6.52$ as it did at $x/c = 5.02$.

The foregoing shows that the vertical component of turbulence decreases in planes close to the free surface. Normally, one would assume that this should be so and that the vertical velocity and turbulence fluctuations must go to zero as a consequence of the free surface boundary. However, the interaction of the vortex with the free surface gives rise to considerable surface signatures (scars and whirls with vertical axes), and the vertical fluctuations need not go to zero as the surface is approached. Nevertheless, one would expect diminishing turbulence intensities, with finite terminal values, as the free surface is approached.

Figure 32 shows the turbulent kinetic energy $E = (u'^2 + v'^2 + w'^2)/2$, normalized by the minimum kinetic energy in each investigator's data, as a function of z/h_0 . As one might expect, E/E_{min} is near maximum on the surface-normal passing through the vortex center. As the free surface is

approached, E/E_{min} decreases sharply at first to about 0.018 (near $z/h_0 = 0.6$), then remains nearly constant up to about $z/h_0 = 0.9$, and then shows a slight increase as $z/h_0 \rightarrow 1$ (the free surface). In other words, the two-dimensionalization of turbulence very near the free surface is not at the expense of total turbulent kinetic energy and that the increase of both u'/U_0 and v'/U_0 is indeed due to the reflection of vertical momentum from the free surface. In this reflection, the free surface behaves as a scarred surface, exhibiting hydrodynamic roughness as it is *seen from below*. Had it behaved like a rigid, *shear-free* boundary, the reflection process would have been relatively simple to interpret. However, the formation of a scar, on the down-flow side of the vortex, the unsteady fluctuations associated with the formation, amalgamation and motion of the whirls (small vortices with axes in the surface-normal direction), and, possibly, the interaction of these scar structures with the fluid (air) directly above render the reflection process much more complex than that in a fully-developed turbulent channel flow (Komori et al., 1982; Rashidi and Banerjee, 1988; Lam and Banerjee, 1992) and require a closer examination of the quasi-coherent turbulent structures near the free surface.

The foregoing raises a number of additional questions which must be addressed if one is to understand the two-dimensionalization process and its role on the formation of SAR images: does E/E_{min} indeed increase very near the free surface, are there other flow situations (not involving a trailing vortex) which exhibit similar characteristics near the free surface, and how do these structures decay with time or downstream distance. Undoubtedly, these questions are rather complicated and their numerical resolution will pose severe tests for all turbulence models.

The transition from fully three-dimensional towards two-dimensional turbulence, the slowing down of the decay of kinetic energy and the strong increase of the length scale have attracted attention in other turbulent flows for a number of years. Jacquin et al. (1989) and the numerous references cited therein dealt with the effect of rotation on the two-dimensionalization of turbulence and the strong departure of the length scales from those for an isotropic state (Brumley, 1984). Hunt and Graham (1978) investigated theoretically the case of homogeneous free stream turbulence impinging upon a rigid wall and found a growing viscous boundary layer adjacent to the free surface and a larger inviscid 'source layer.' At the edge of the viscous surface layer the kinetic energy of turbulence is the same as in the bulk of the fluid, but the fluid velocity component normal to the surface vanishes and the energy in this motion is partitioned (equally, for an isotropic flow) to the streamwise and lateral motions.

Loewen et al. (1986) investigated the statistics of free-surface flow structures generated by a vertical bar grid moving through water in a towing tank. They have found a profusion of coherent surface structures that either rotate (surface eddies), translate (river flow), or are relatively stagnant and that the surface flow is predominantly two dimensional. Their results show that the eddy size distribution gradually shifts to larger size as turbulence decays and an increasing fraction of the fluctuating kinetic energy is transferred into 'rivers'. Brumley (1984) and Dickey (1984), made turbulence measurements near the free surface in grid-stirred tanks and demonstrated that the true dissipation rate is relatively uniform near the surface, rather than decaying as the fourth power of the distance from the horizontal grid, as it does in the case of deeply-submerged grids. Sarpkaya and Suthon (1991) suggested, on the basis of their observations, that the free surface turbulence

exhibits features that obey the decay laws of two-dimensional turbulence. Subsequently, Sarpkaya (1992a, 1992b) has simulated the evolution of near-surface structures by a decaying 2-D turbulence through vortex dynamics and has shown that the energy and enstrophy inertial ranges coexist, with an upscale energy transfer (reverse energy cascade) and downscale enstrophy transfer in the same wavenumber interval while conserving energy and enstrophy.

Komori et al. (1982) made measurements of temperature, velocity, and turbulence fields very close to the free surface in an open channel flow and found that the vertical motions are damped while the streamwise and spanwise motions are promoted. Subsequently, Rashidi and Banerjee (1988) and Lam and Banerjee (1992) found, through flow visualizations of bubble streaks near the free surface of an open-channel flow and also through numerical simulations, that the kinetic energy of turbulence is redistributed from the surface-normal to the parallel fluctuations. Their results are quite similar to those obtained by Komori et al. (1982) in the range where they may be compared. Lam and Banerjee (1992) noted that unlike the numerical prediction, the experimental values of w' did not vanish at the interface. They have suggested that "this was probably due to the slight waves present in the experiments." As noted earlier, these experiments are for relatively simple channel flows, containing no trailing vortices or jets.

More recently, Anthony (1990) and Anthony and Willmarth (1992) made turbulence measurements in a round jet beneath a free surface and found that near the surface u'/U_0 and v'/U_0 increase while w'/U_0 decreases. Their E/E_{min} data (Anthony and Willmarth, 1992), calculated from their Fig. 4b, are shown in Fig. 32 together with those calculated from the RMS data of Lam and Banerjee (1992), Komori et al. (1982) and the present investigation.

In doing so, the vertical distance (from the channel bottom, the jet axis, or the vortex axis) was expressed in terms of the relative distance z/h_0 . The turbulent kinetic energy for each case was scaled by its corresponding minimum value. This normalization does not imply identical scaling laws but allows one to compare the decay of E/E_{\min} for the four sets of data considered herein.

The conclusion common to all of the foregoing studies is that the free surface redistributes part or all of the normal turbulent kinetic energy $w'^2/2$ into the streamwise and spanwise components $u'^2/2$ and $v'^2/2$. The turbulent kinetic energy increases very near the free surface in all of the four sets of data. The results for the channel and vortex flows [Lam and Benarjee (1992), Komori et al. (1982, 1993), and the present data] show for $z/h_0 > 0$ that the values of E/E_{\min} decrease by comparable rates and then acquire nearly constant values in a very thin layer near the free surface. This lends credence to Sarpkaya's (1992a, 1992b) and Sarpkaya and Suthon's (1991) numerical simulation of the evolution of near-surface structures by a decaying 2-D turbulence via vortex dynamics (see, e.g., Sarpkaya, 1989). The case of the round jet parallel to the free surface is an exception where the turbulent kinetic energy remains nearly constant throughout the region above the jet axis. Apparently, the dynamics of turbulence very close to the free surface (as $z/h_0 \rightarrow 1$) is very complex and significantly different from that near a smooth or rough rigid surface. The role of the near-surface layer, the persistence of u'/U_0 and v'/U_0 as $z/h_0 \rightarrow 1$, the interaction between quasi-two-dimensional coherent structures near the free surface and the restructuring and modulation of this interaction by wind and contaminants need extensive measurements.

IV. CONCLUSIONS

1. The interaction of a single turbulent trailing vortex with a deformable free surface has been undertaken for the purpose of exploring the velocity and turbulence field in the vicinity of a clean free surface. The evidence presented herein shows that there are two regions wherein one, near the vortex, the turbulent kinetic energy decays rapidly with increasing vertical distance, and in the other, very near the free surface (in the order of millimeters), the said energy remains essentially constant. The energy of the vertical velocity fluctuations is redistributed among the lateral and streamwise motions. Even though all four flows discussed herein exhibit, to varying degrees of intensity, the behaviors noted above, trailing vortices and open channel flows delineate the two distinct regions of turbulent energy distribution more emphatically than submerged jets. Finally, it is noted that the results of the present investigation lend further credence to the numerical simulation of the free surface structures via two-dimensional vortex dynamics.

2. The use of a turbulent vortex near the free surface of an otherwise smooth uniform flow proved to be a 'kernel' experiment towards the elucidation of the dynamical processes in vorticity/free-surface interaction. Detailed measurements of mean velocity and all components of the Reynolds stress tensor are needed towards the development of a predictive model of the vorticity/free-surface interaction. These measurements and the understanding of the character of the quasi-coherent structures near the free surface constitute the essence of the on-going investigation.

APPENDIX

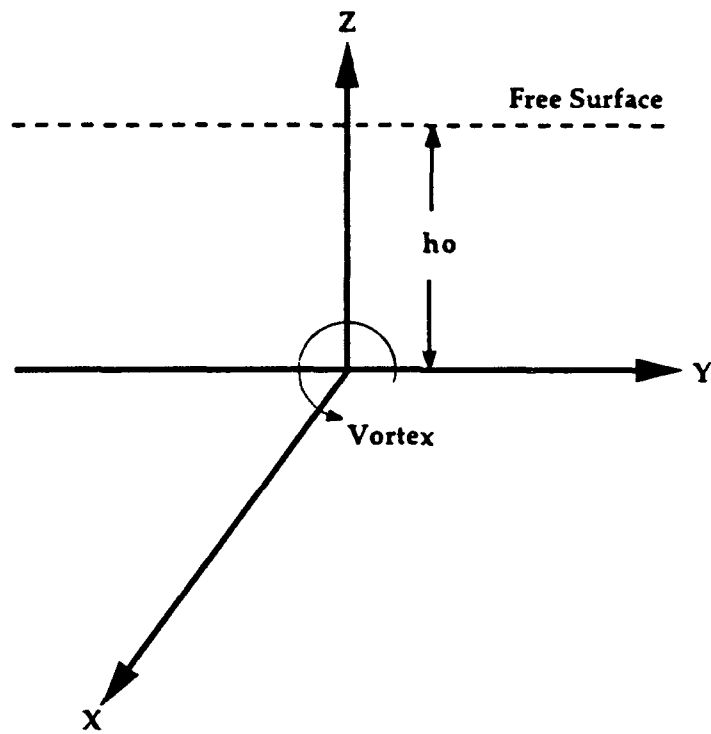


Figure 1. Definition Sketch

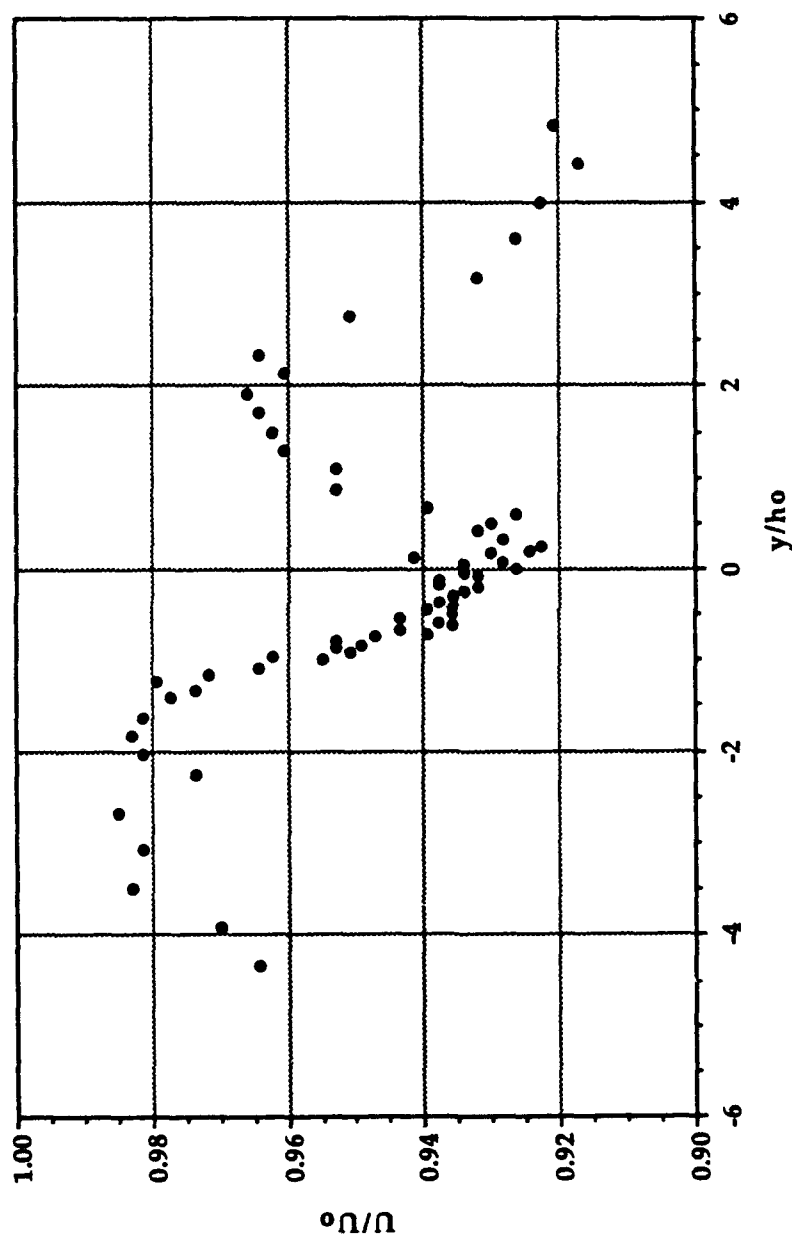


Figure 2. U/U_o versus Lateral Distance for $Z/h_o = 0.58$ and $x/c = 5.02$

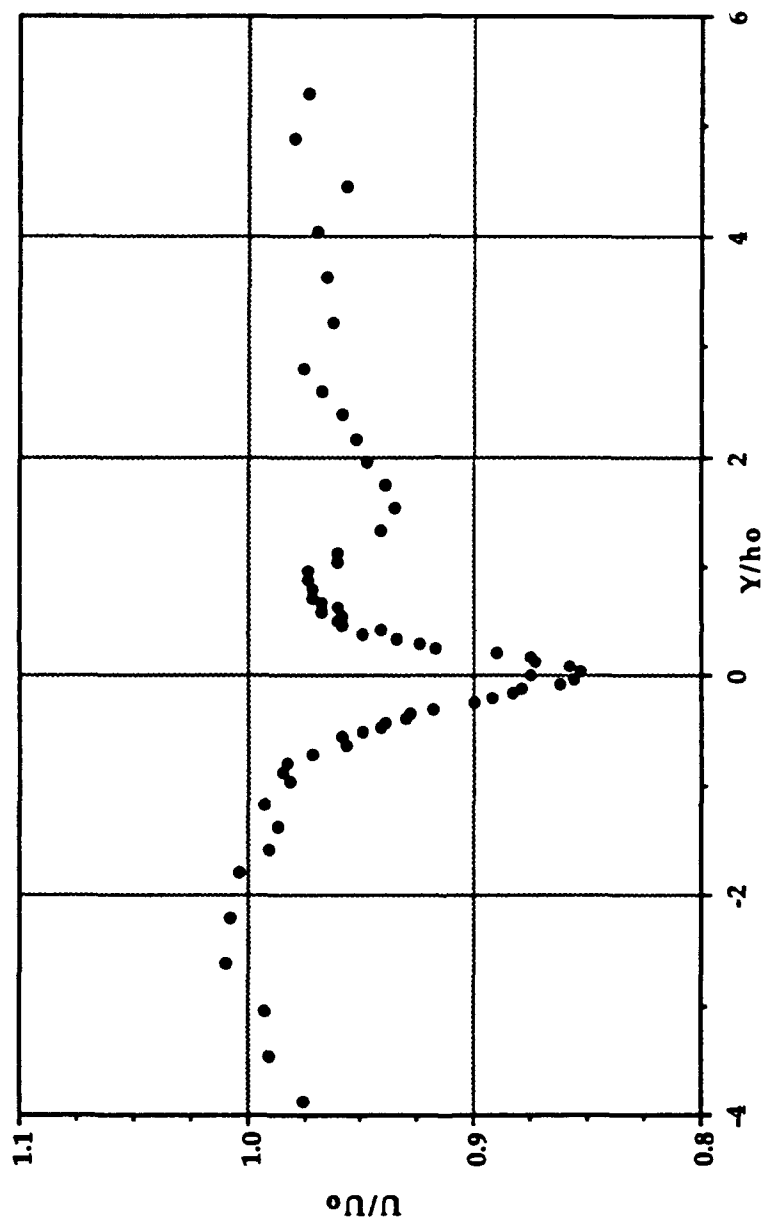


Figure 3. U/U_0 versus Lateral Distance for $Z/h_0 = 0.00$ and $x/c = 5.02$

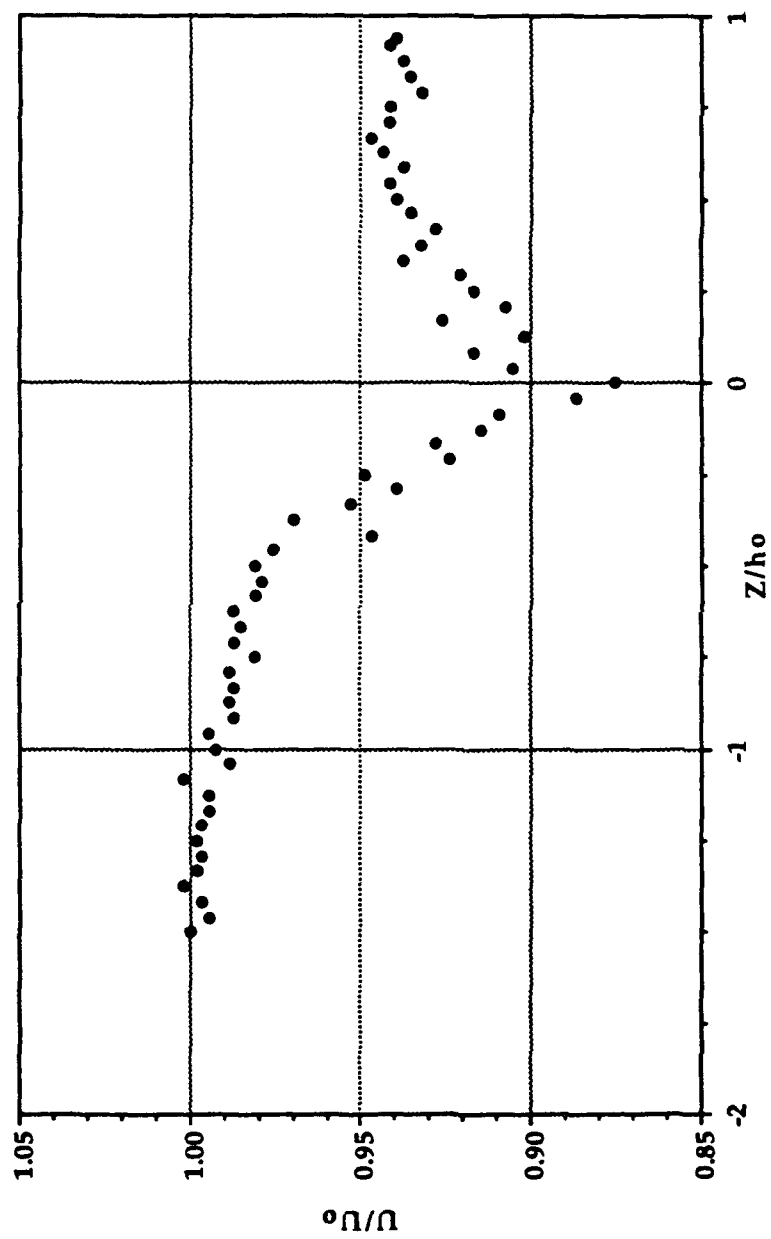


Figure 4. U/U_o versus Vertical Distance for $Y/h_0 = -0.27$ and $x/c = 5.02$

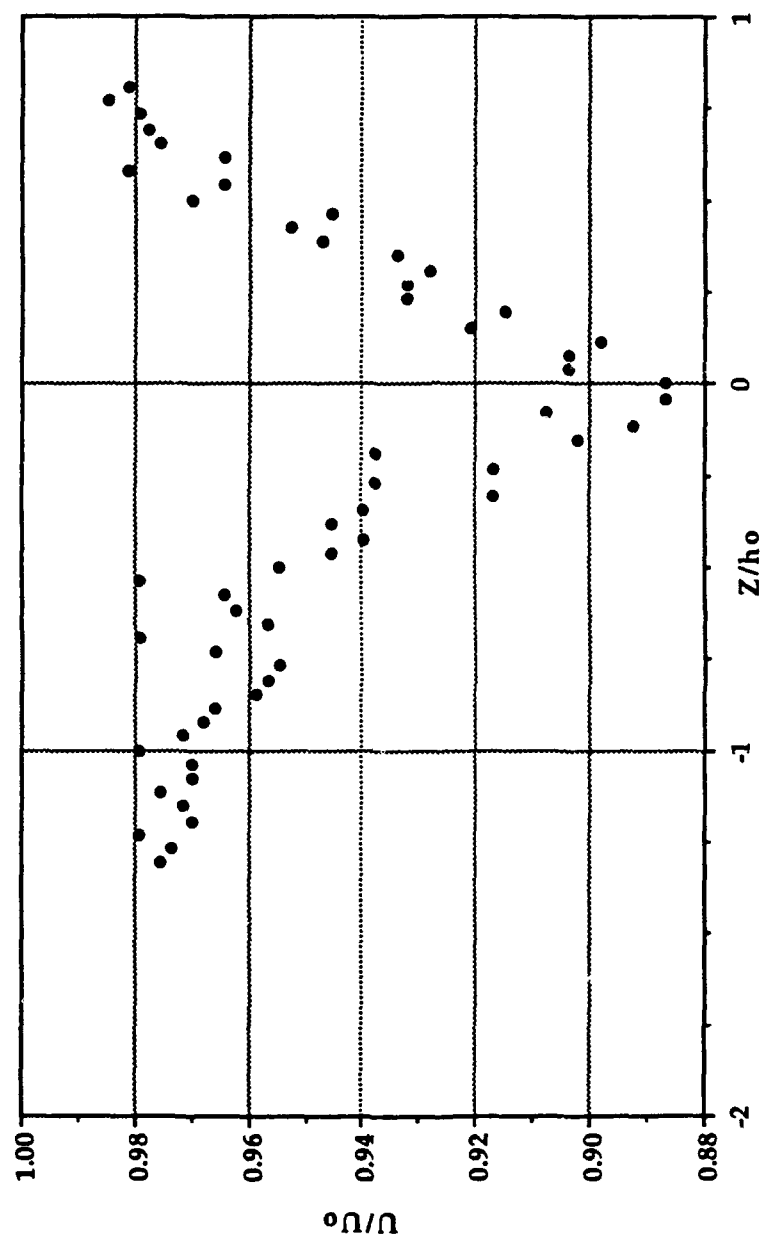


Figure 5. U/U_0 versus Vertical Distance for $Y/h_0 = 0.00$ and $x/c = 5.02$

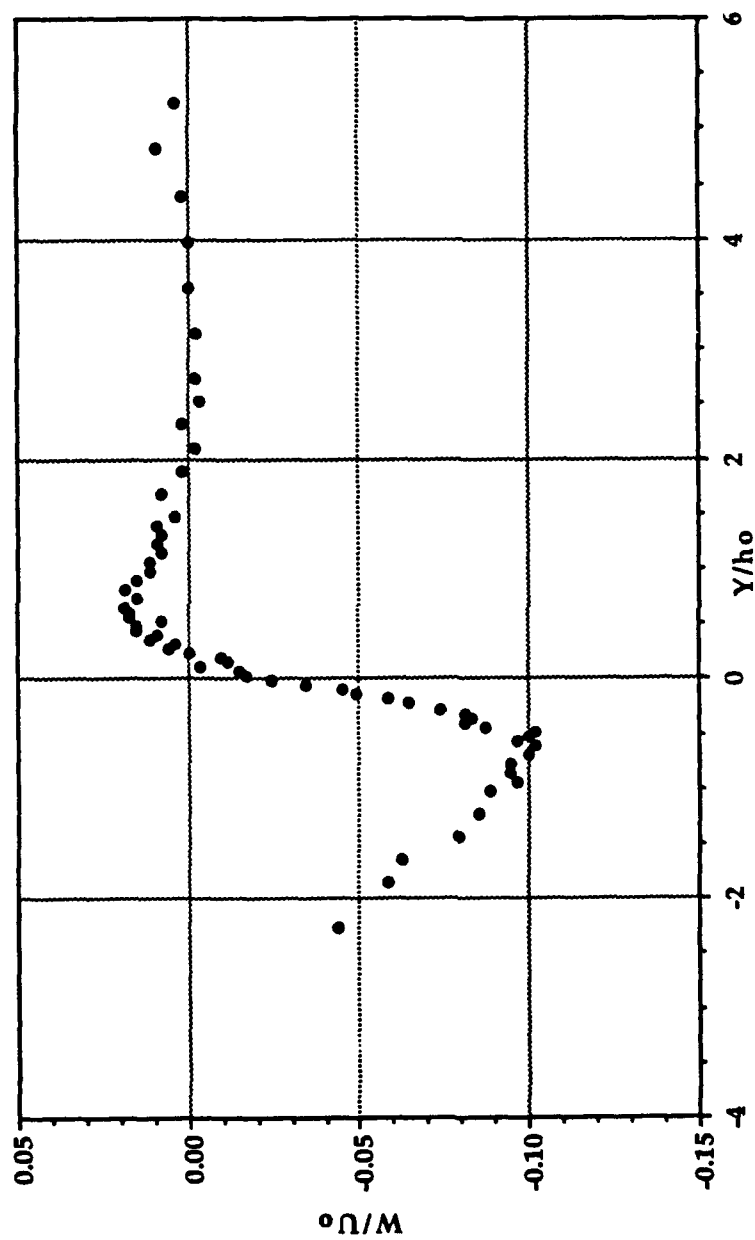


Figure 6. W/U_0 versus Lateral Distance for $Z/h_0 = 0.38$ and $x/c = 5.02$

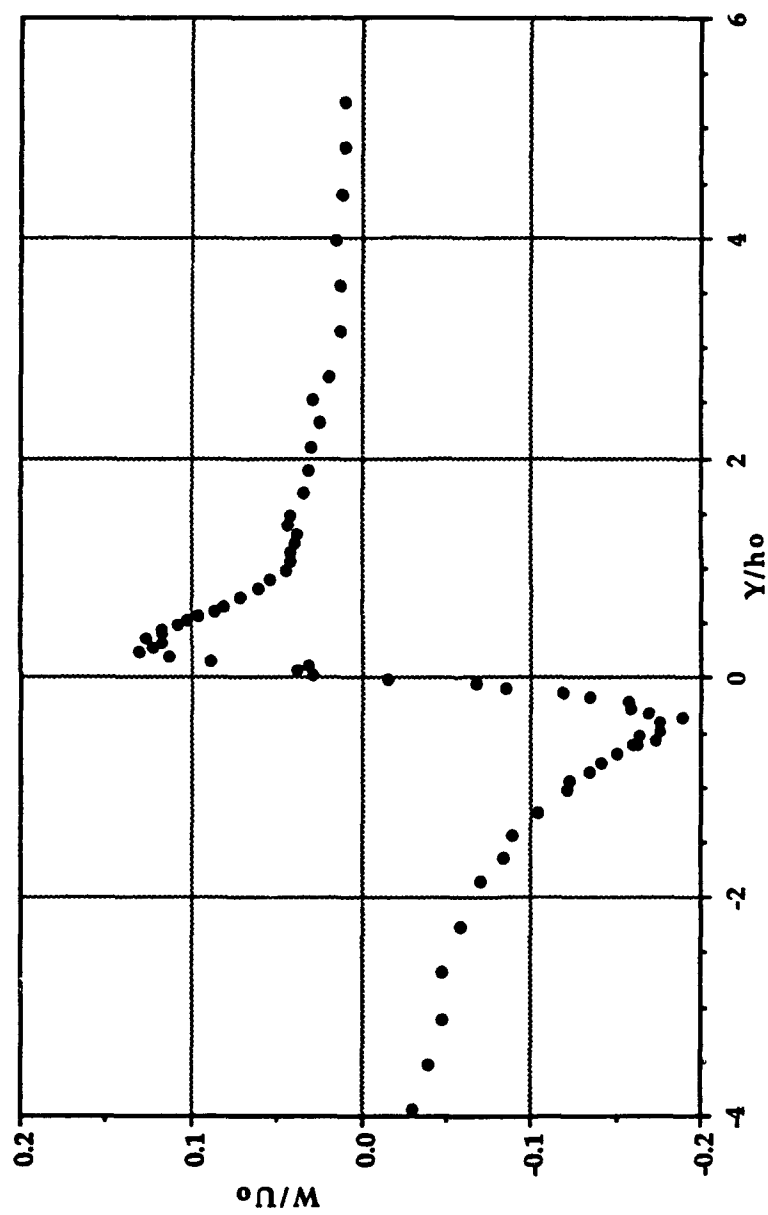


Figure 7. W/U_o versus Lateral Distance for $Z/h_o = 0.00$ and $x/c = 5.02$

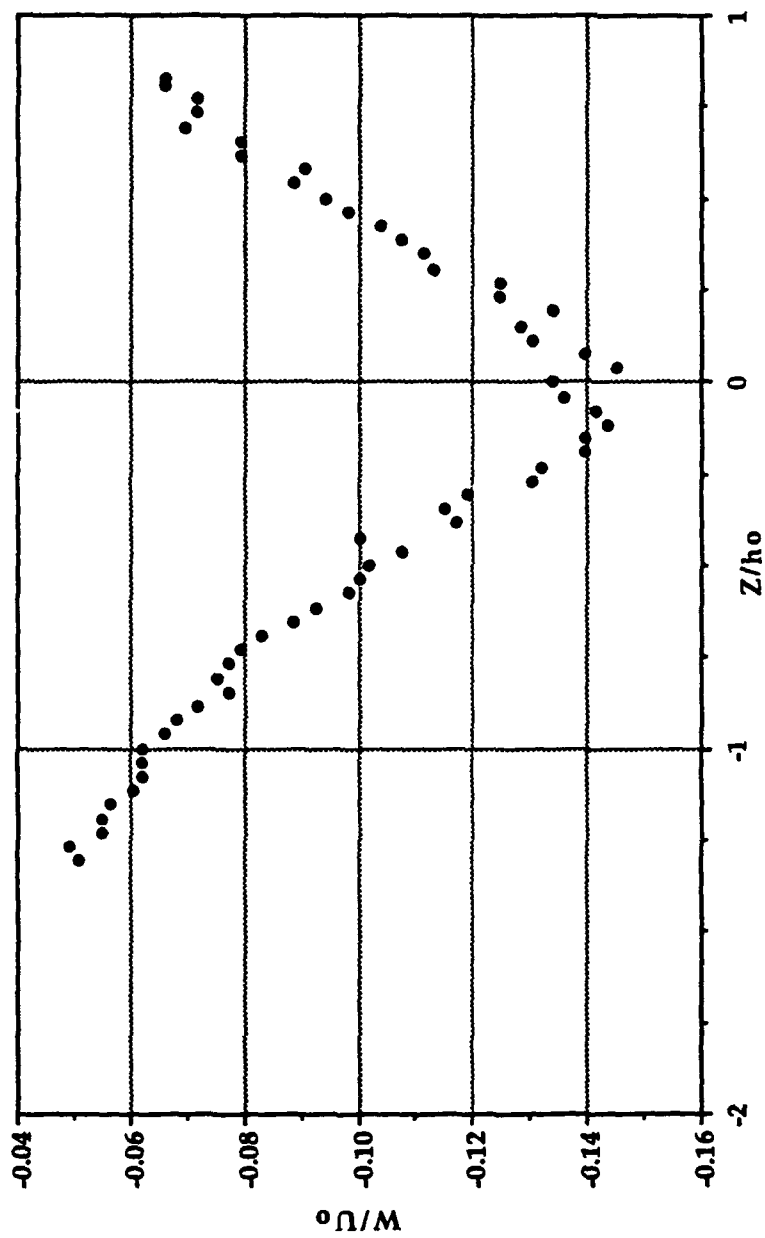


Figure 8. W/U_0 versus Vertical Distance for $Y/h_0 = -0.40$ and $x/c = 5.02$

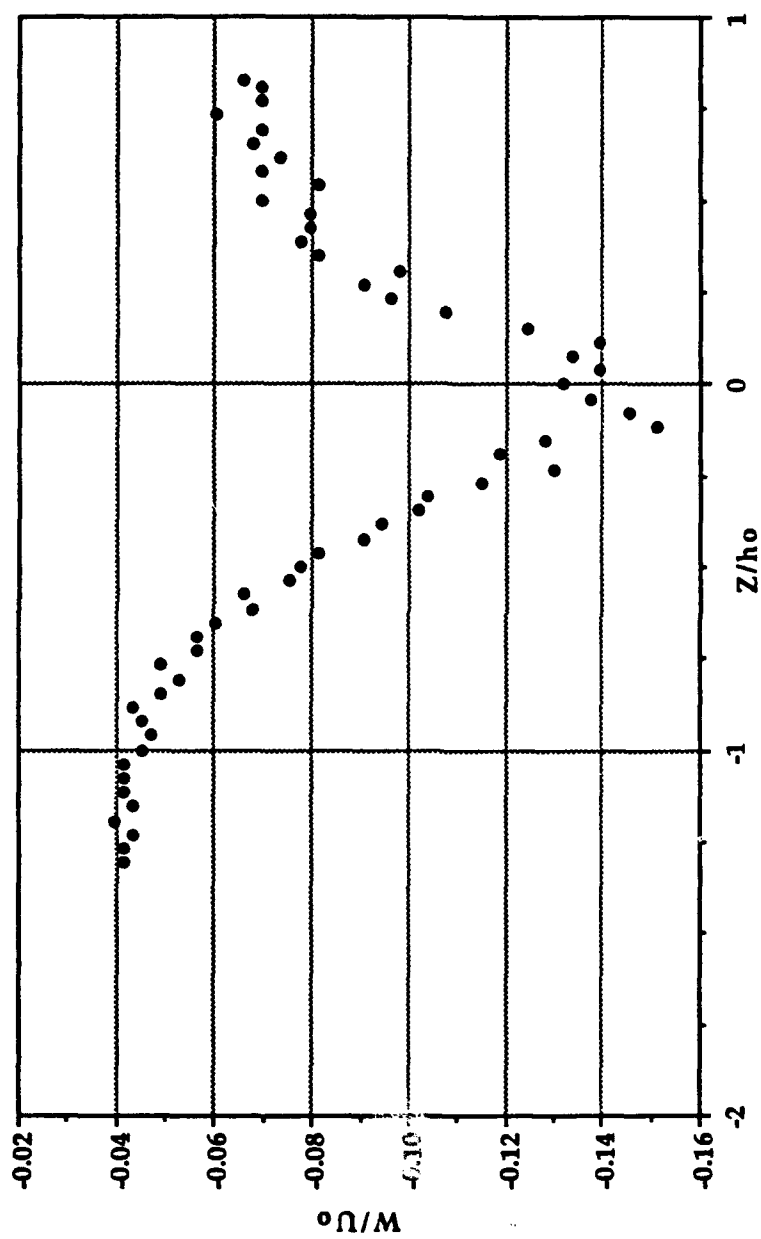


Figure 9. W/U_0 versus Vertical Distance for $Y/h_0 = -0.27$ and $x/c = 5.02$

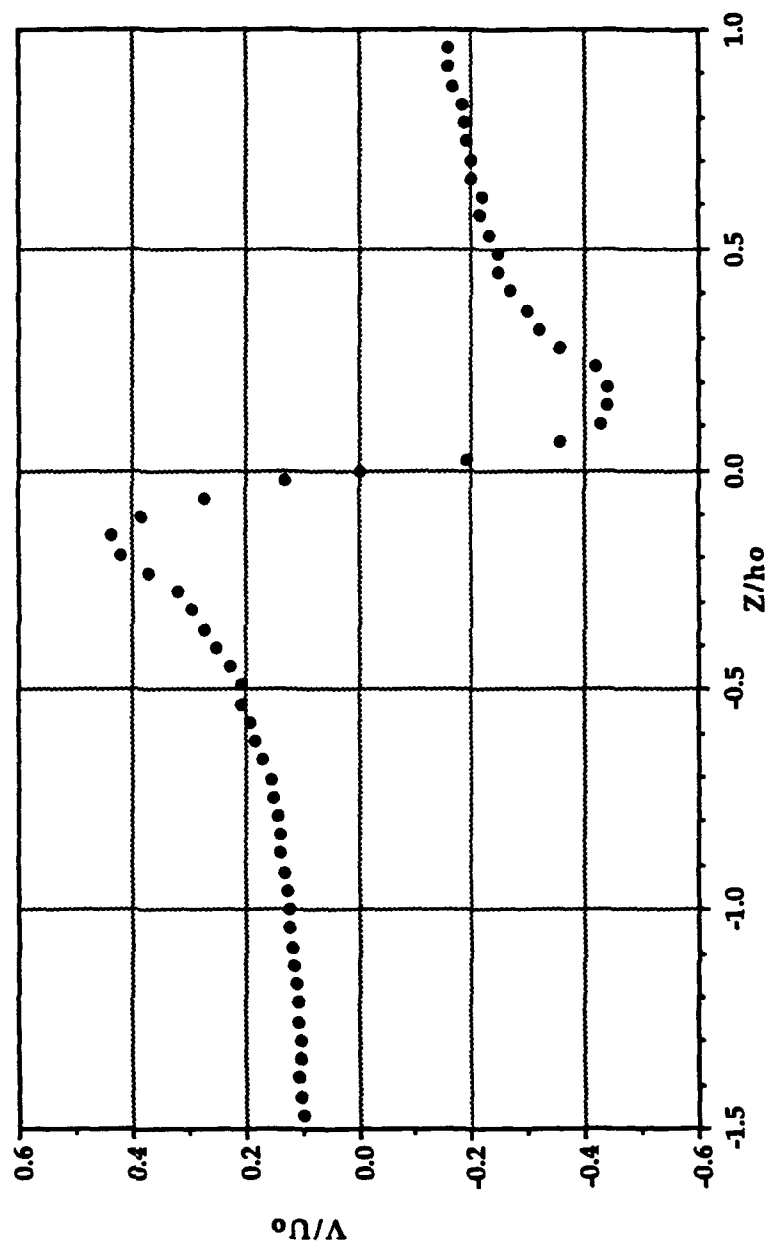


Figure 10. V/U_0 versus Vertical Distance for $Y/h_0 = 0.00$ and $x/c = 5.02$

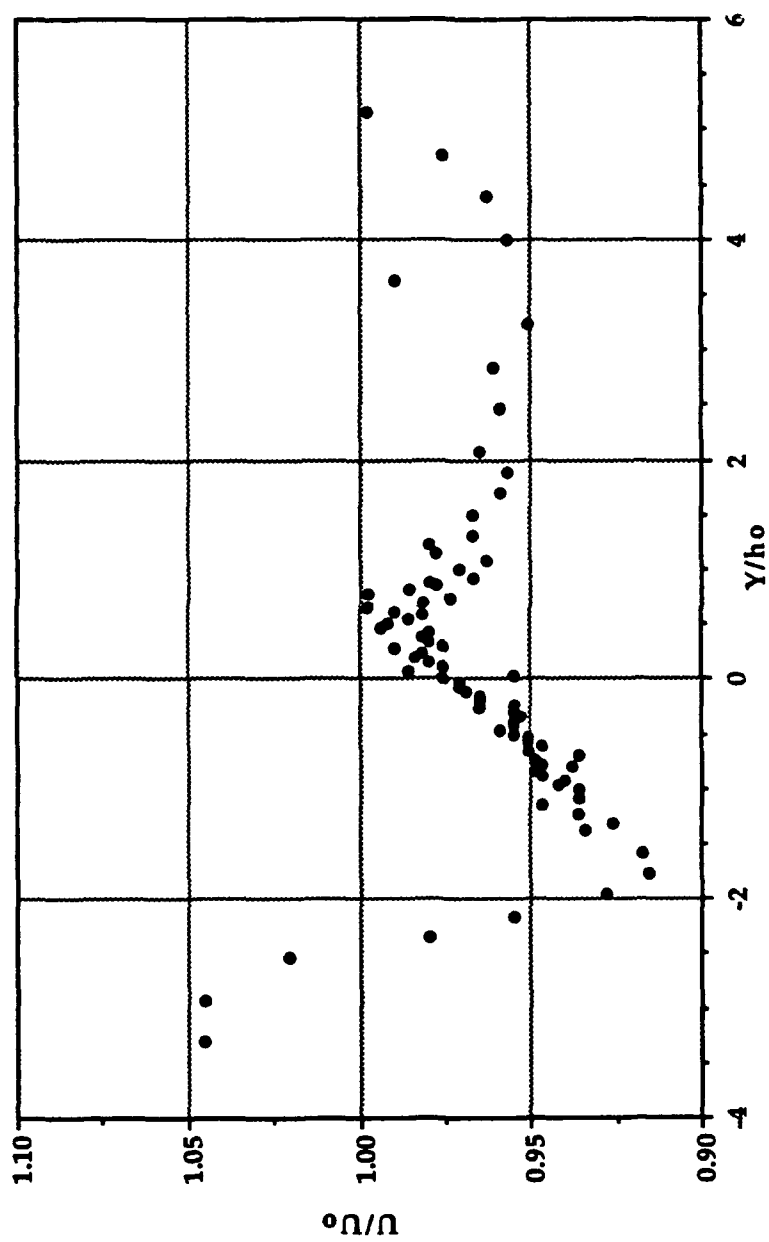


Figure 11. U/U_o versus Lateral Distance for $Z/h_o = 0.85$ and $x/c = 6.52$

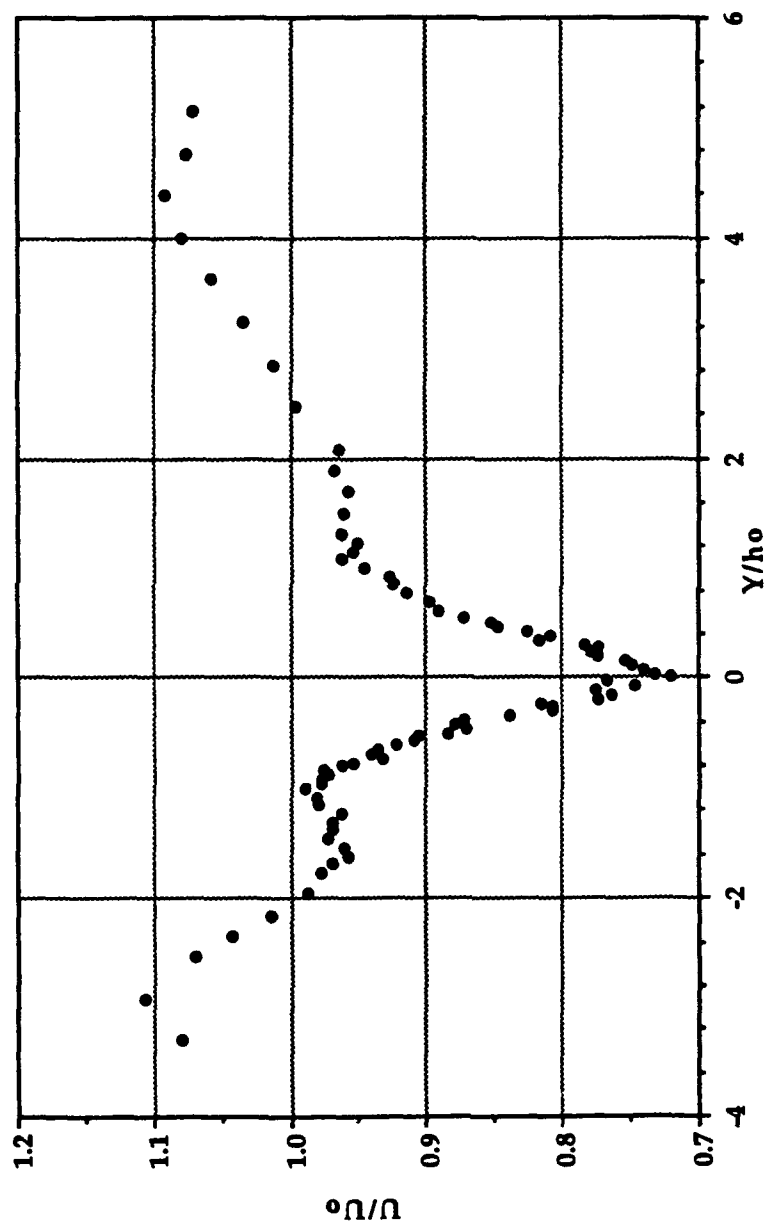


Figure 12. U/U_o versus Lateral Distance for $Z/h_o = 0.00$ and $x/c = 6.52$

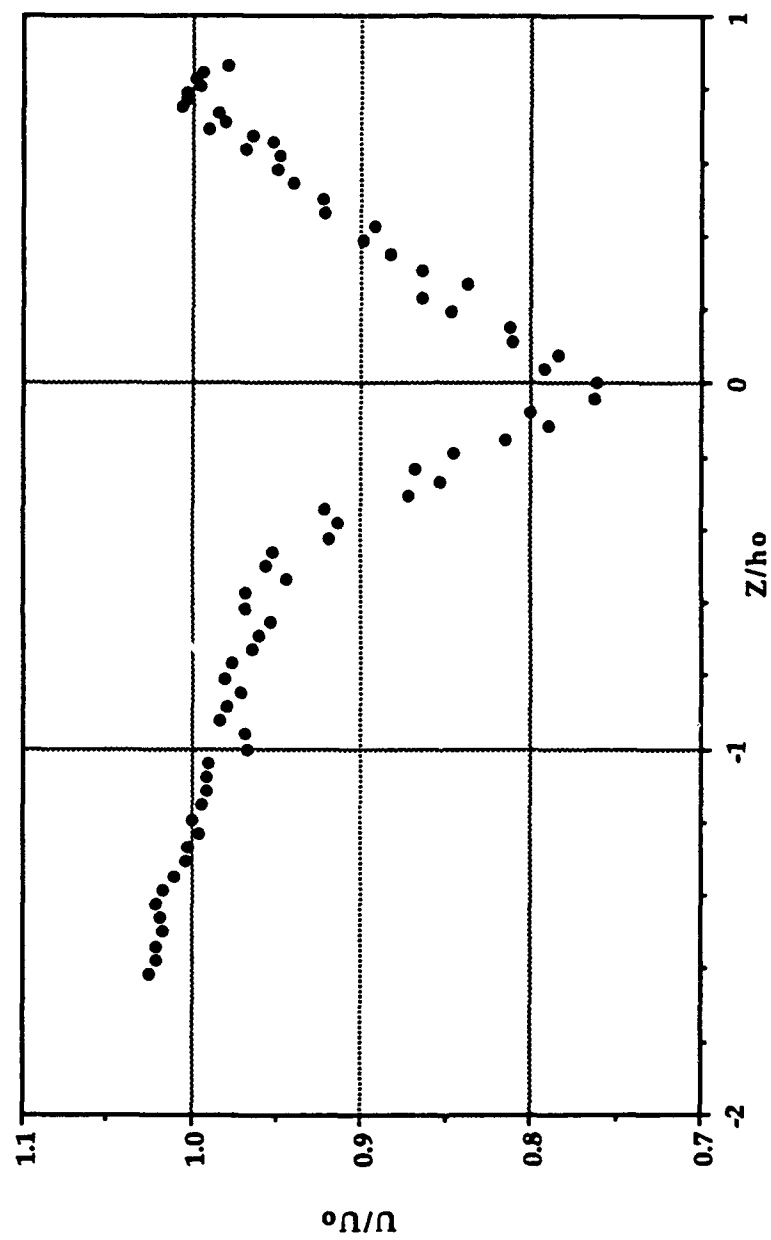


Figure 13. U/U_o versus Vertical Distance for $Y/h_o = -0.46$ and $x/c = 6.52$

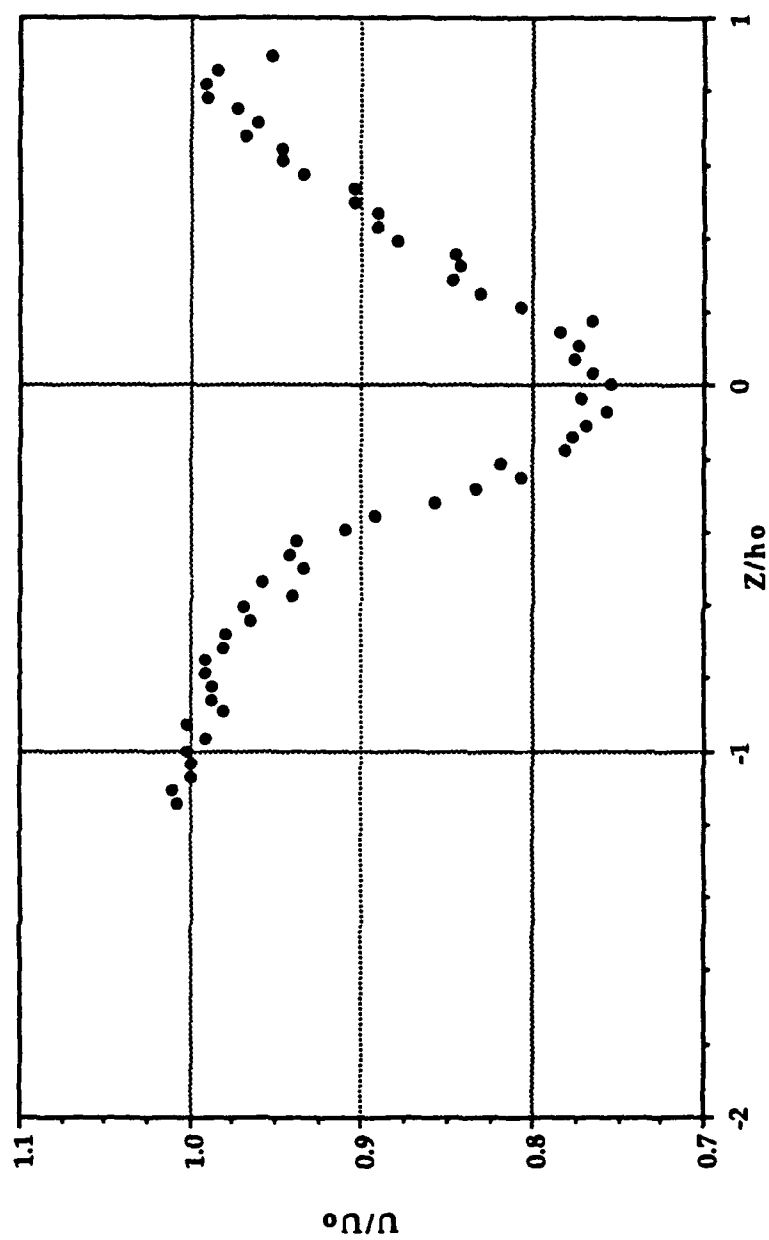


Figure 14. U/U_o versus Vertical Distance for $Y/h_o = 0.25$ and $x/c = 6.52$

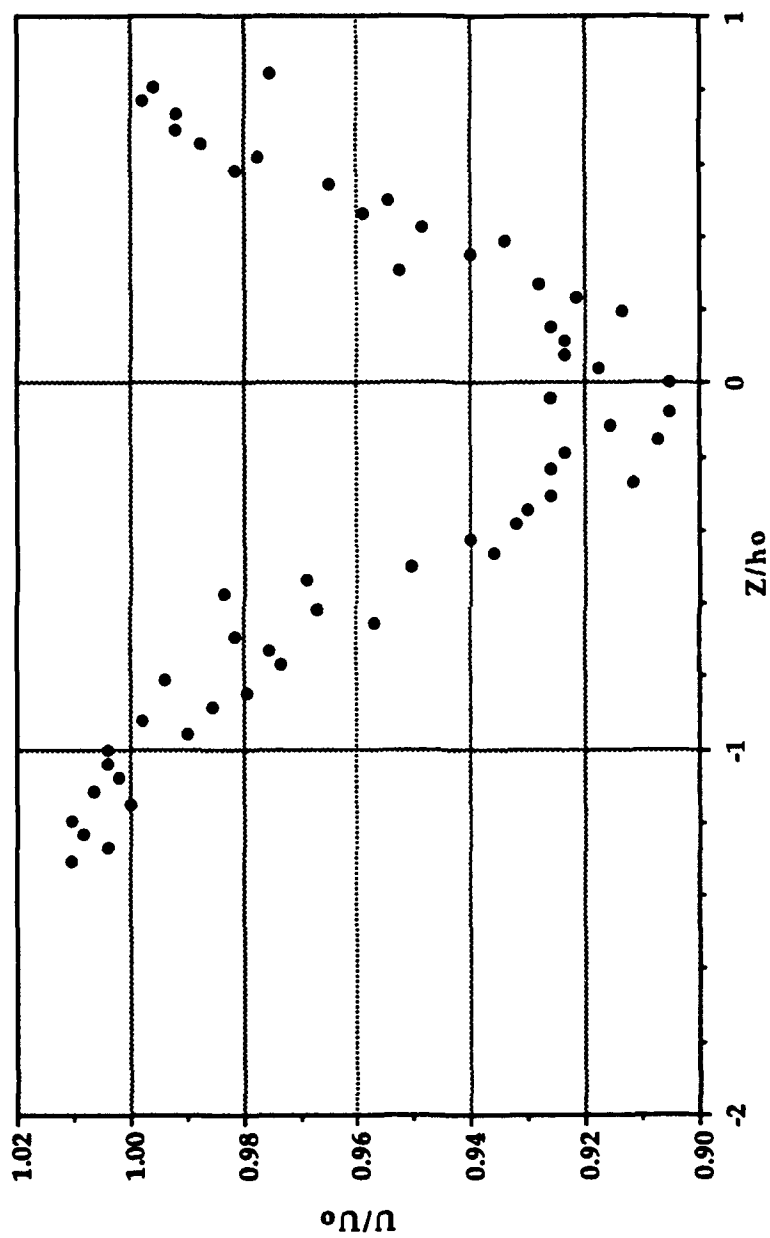


Figure 15. U/U_o versus Vertical Distance for $Y/h_o = 0.65$ and $x/c = 6.52$

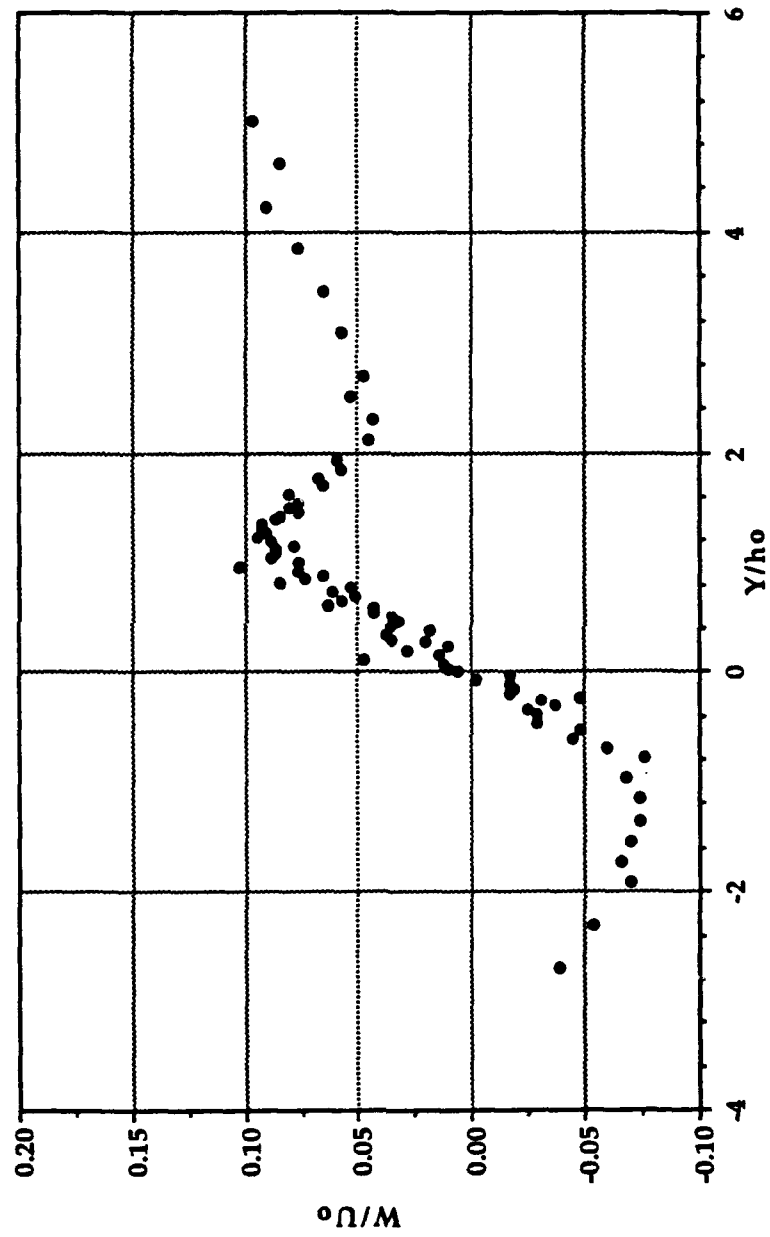


Figure 16. W/U_0 versus Lateral Distance for $Z/h_0 = 0.85$ and $x/c = 6.52$

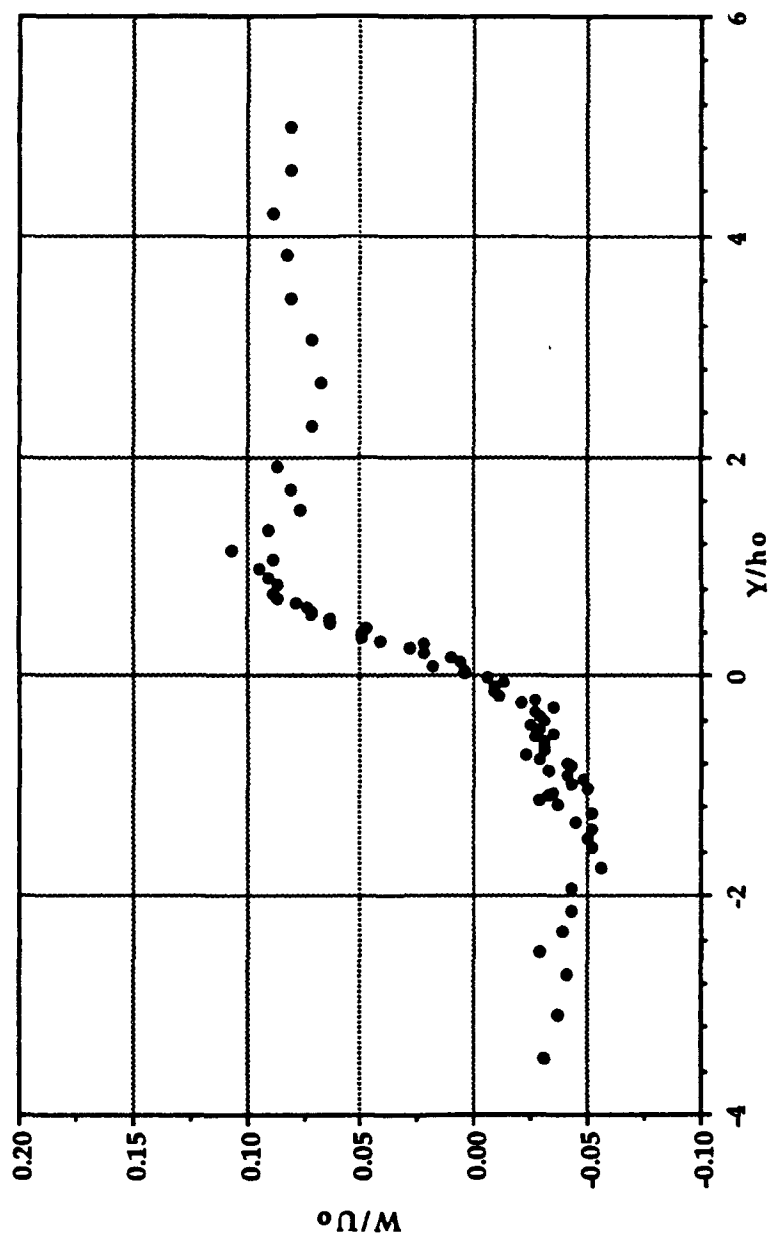


Figure 17. W/U_0 versus Lateral Distance for $Z/h_0 = 0.62$ and $x/c = 6.52$

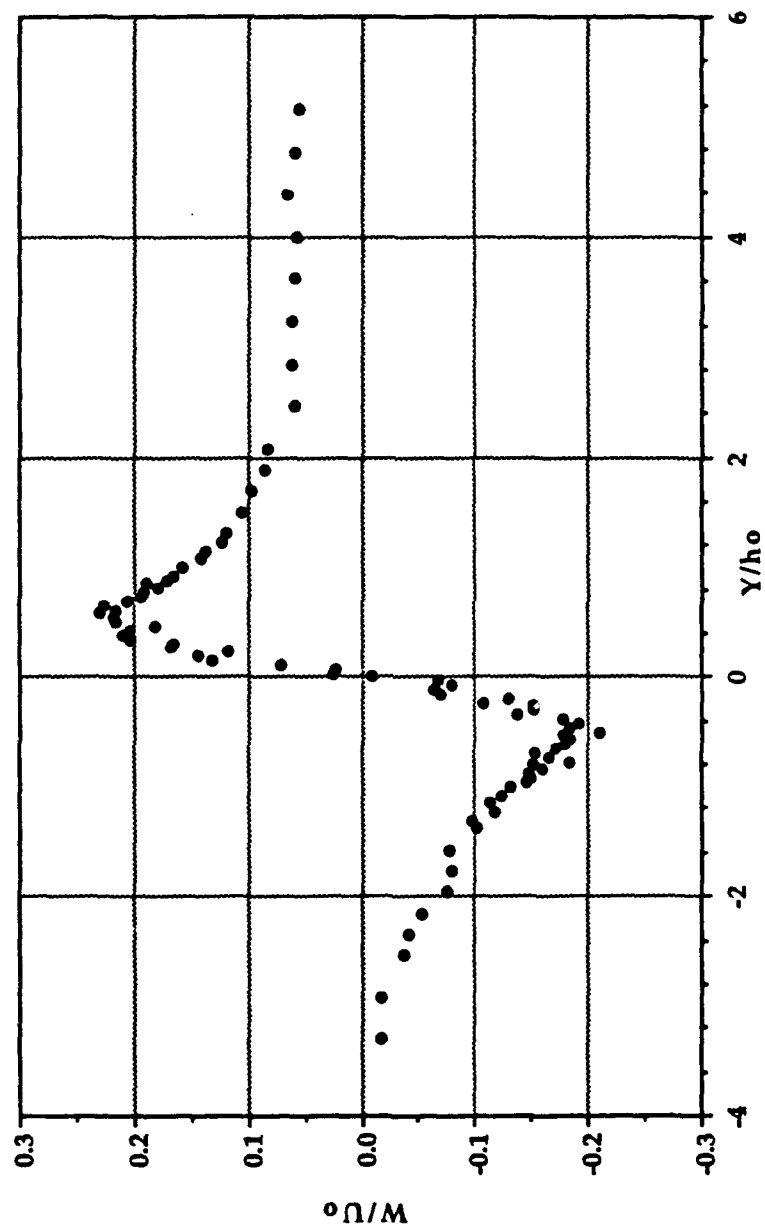


Figure 18. W/U_o versus Lateral Distance for $Z/h_o = 0.00$ and $x/c = 6.52$

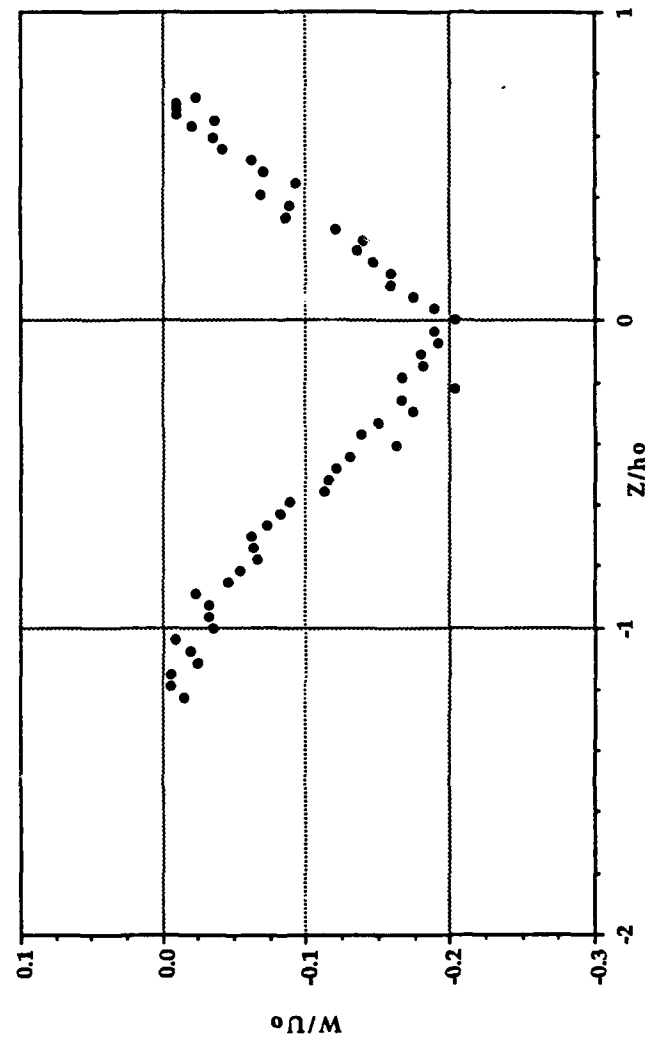


Figure 19. W/U_o versus Vertical Distance for $Y/h_o = -0.44$ and $x/c = 6.52$

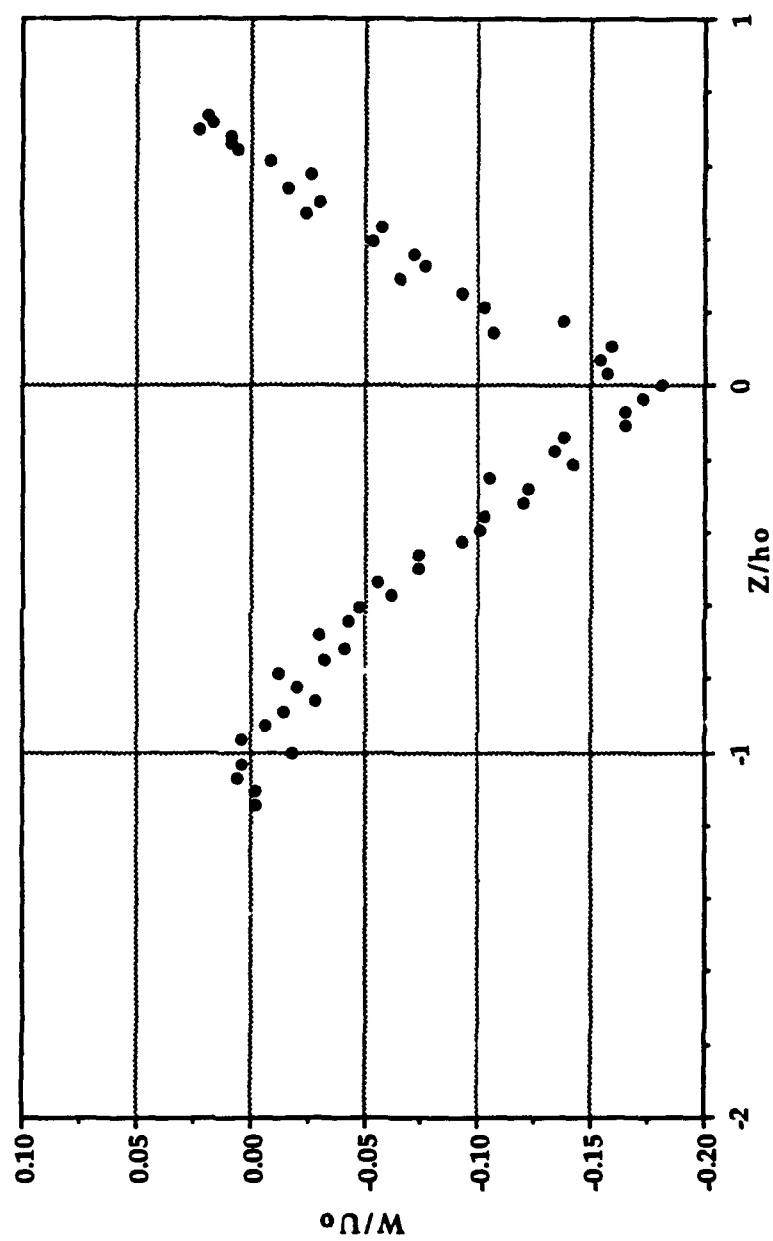


Figure 20. W/U_0 versus Vertical Distance for $Y/h_0 = -0.25$ and $x/c = 6.52$

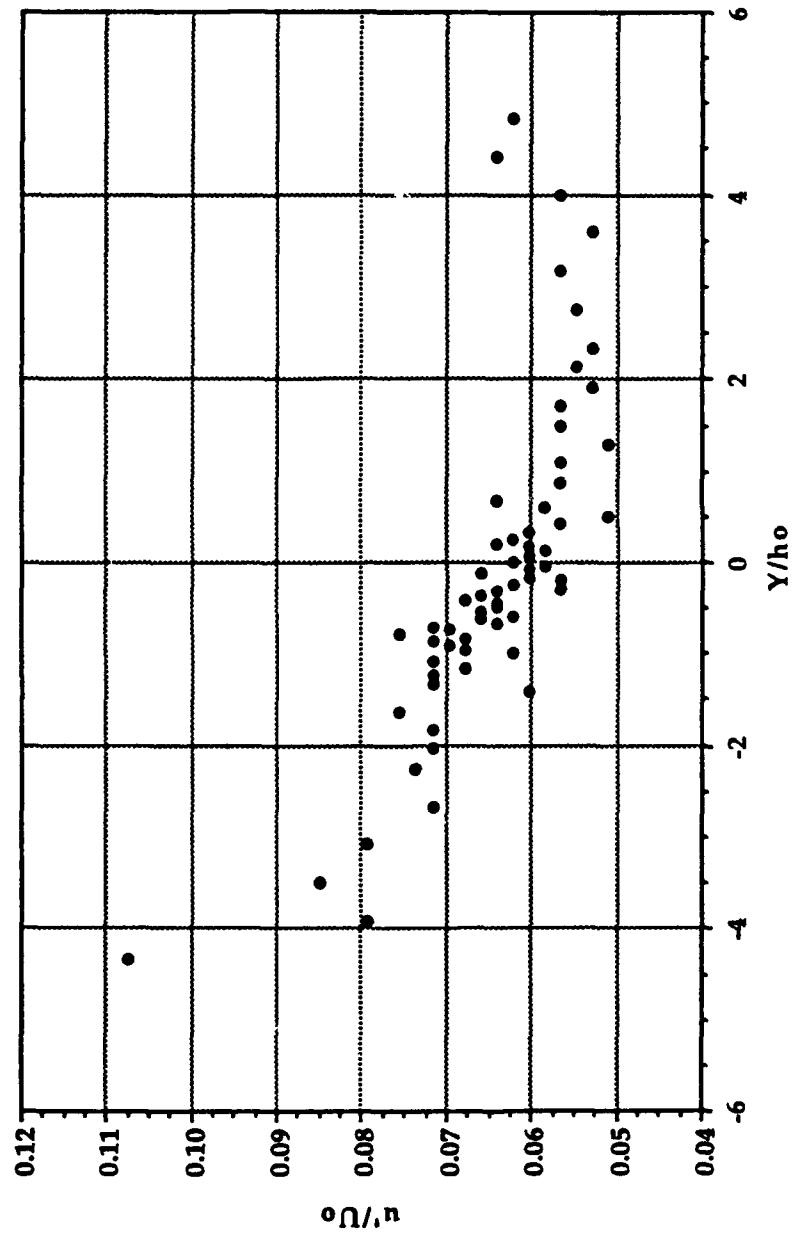


Figure 21. u'/U_o versus Lateral Distance for $Z/h_o = 0.60$ and $x/c = 5.02$

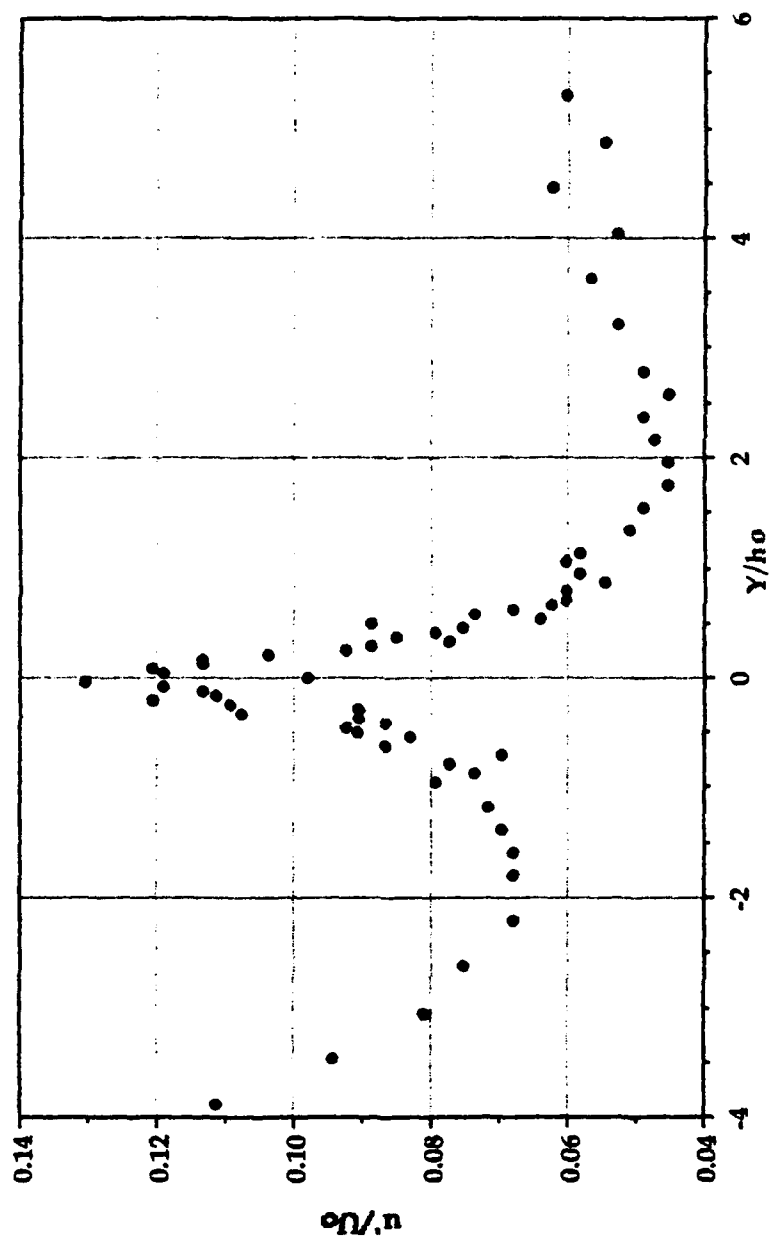


Figure 22. u'/U_o versus Lateral Distance for $Z/h_0 = 0.00$ and $x/c = 5.02$

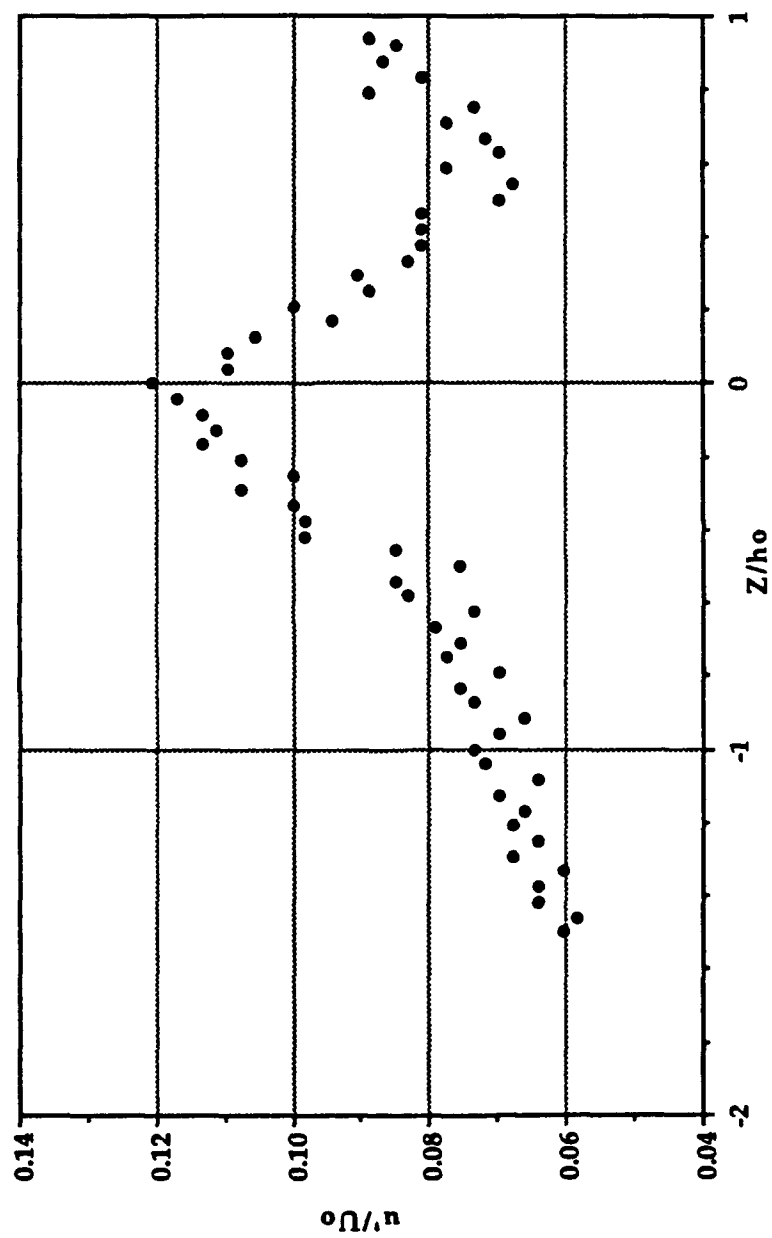


Figure 23. u'/U_o versus Vertical Distance for $Y/h_o = -0.27$ and $x/c = 5.02$

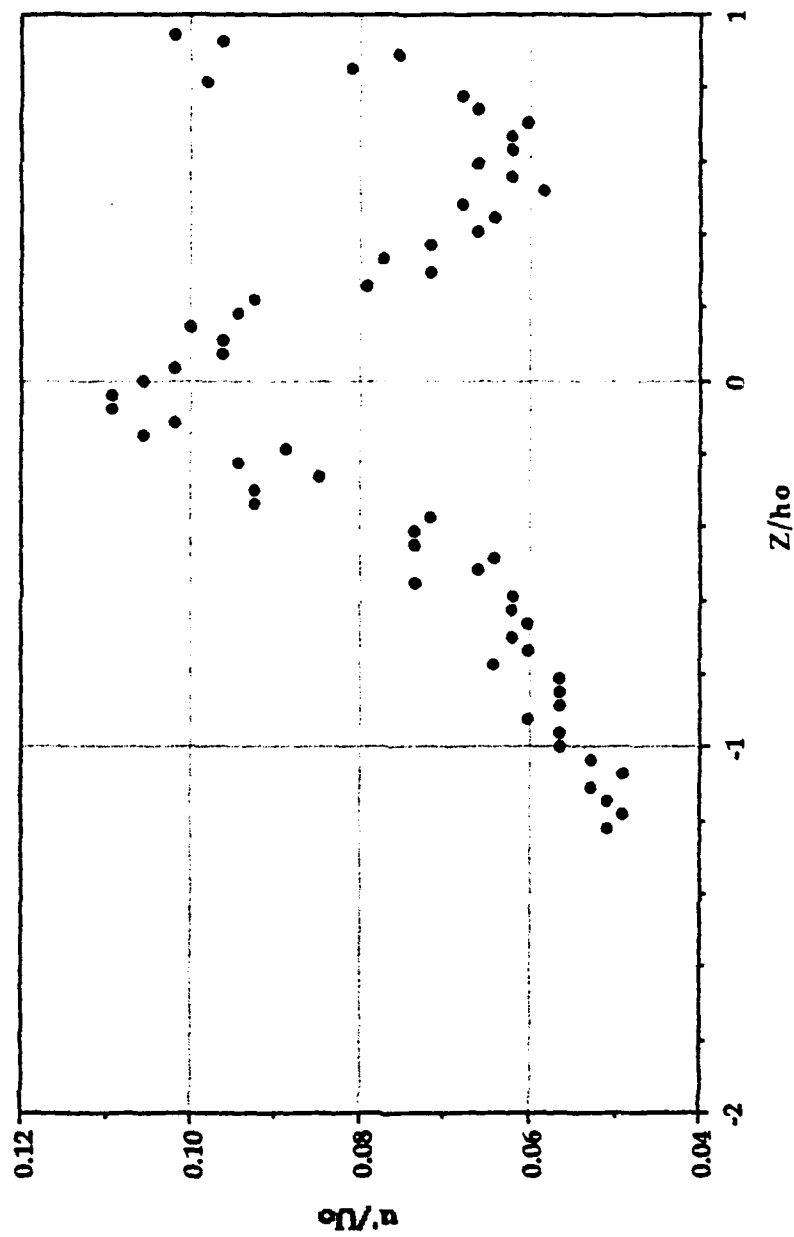


Figure 24. u'/U_o versus Vertical Distance for $Y/h_0 = 0.60$ and $x/c = 5.02$

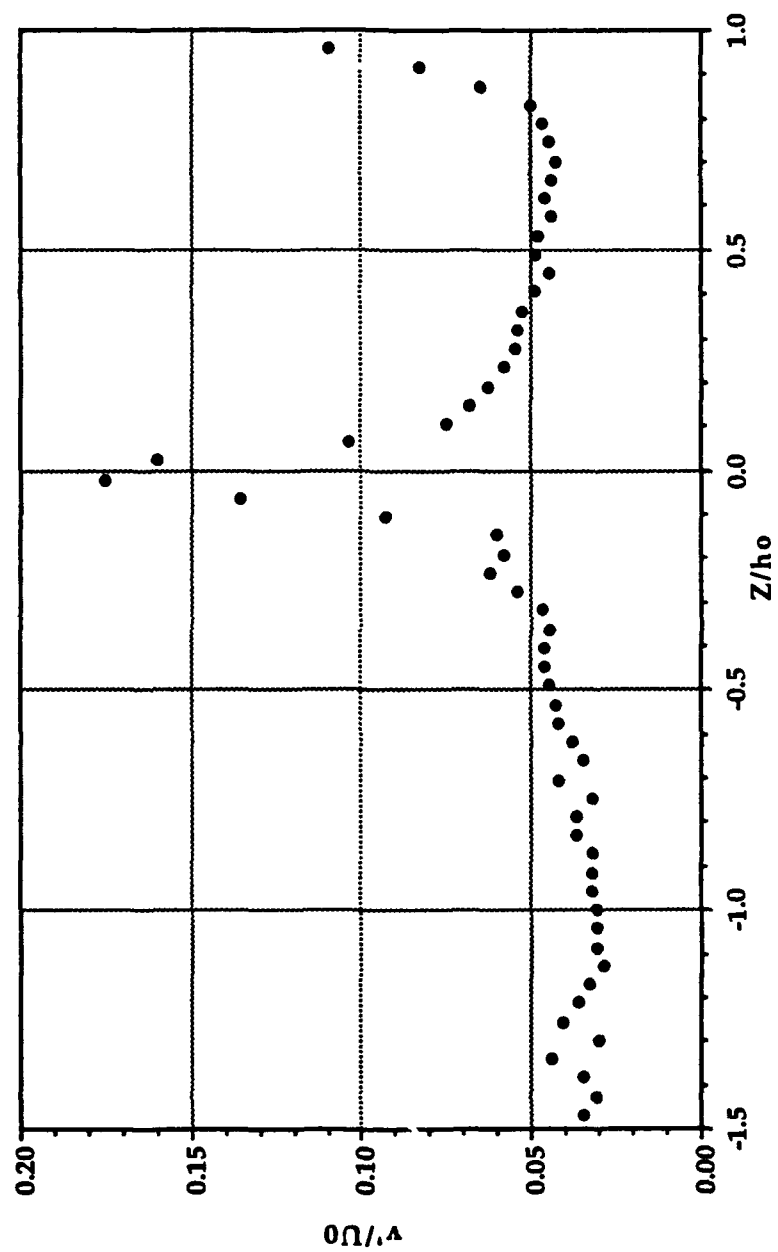


Figure 25. v'/U_o versus Vertical Distance for $Y/h_o = 0.00$ and $x/c = 5.02$

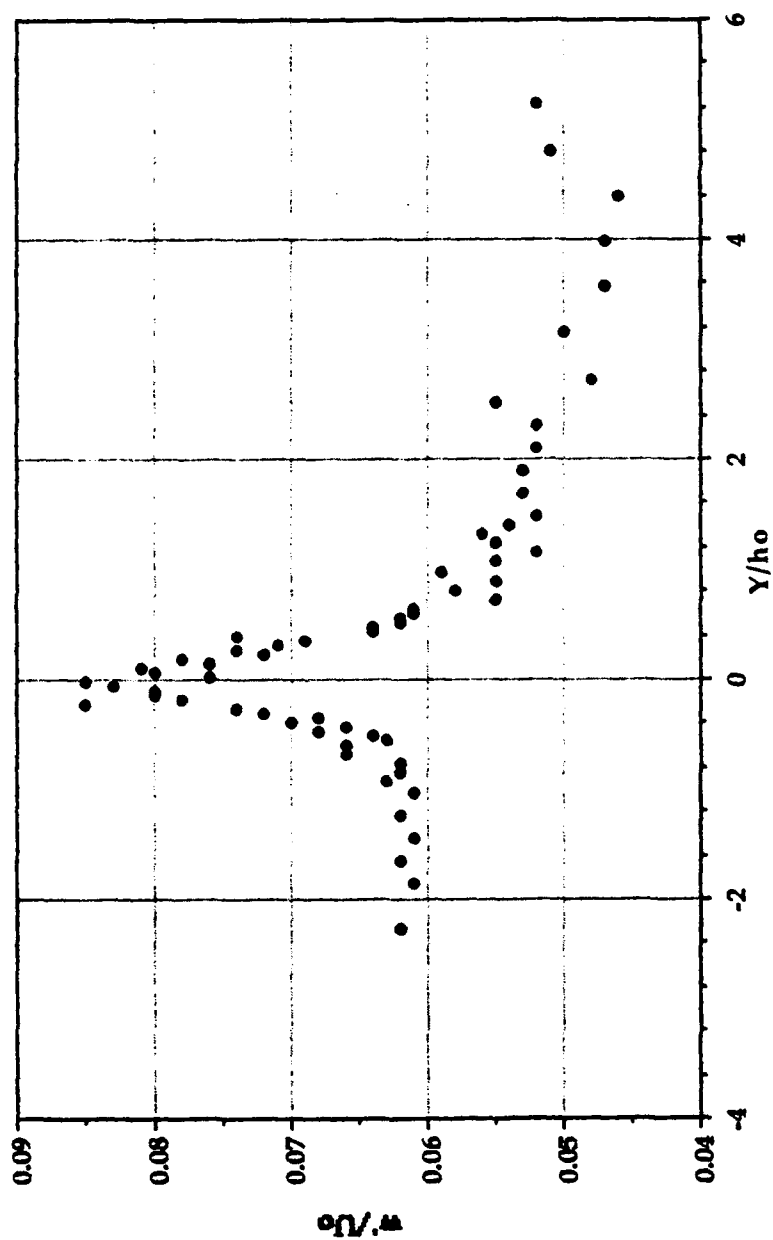


Figure 26. w'/U_o versus Lateral Distance for $Z/h_o = 0.38$ and $x/c = 5.02$

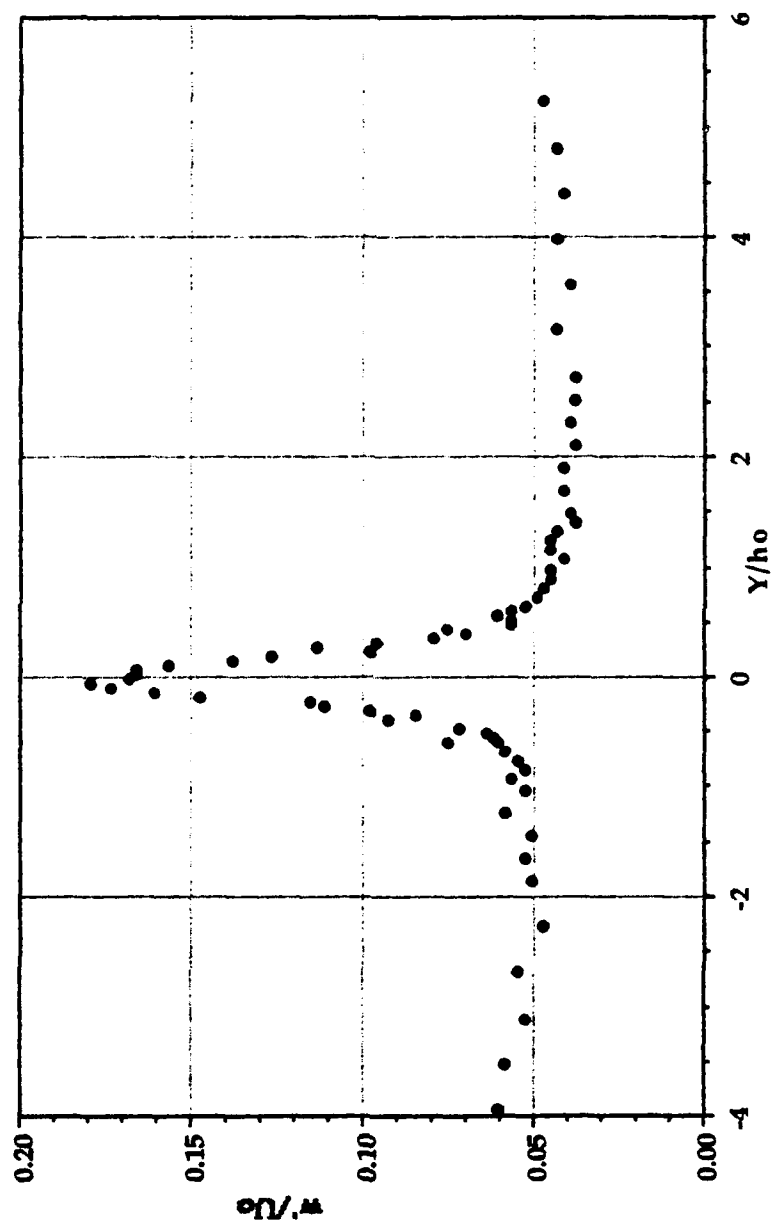


Figure 27. w'/U_o versus Lateral Distance for $Z/h_o = 0.00$ and $x/c = 5.02$

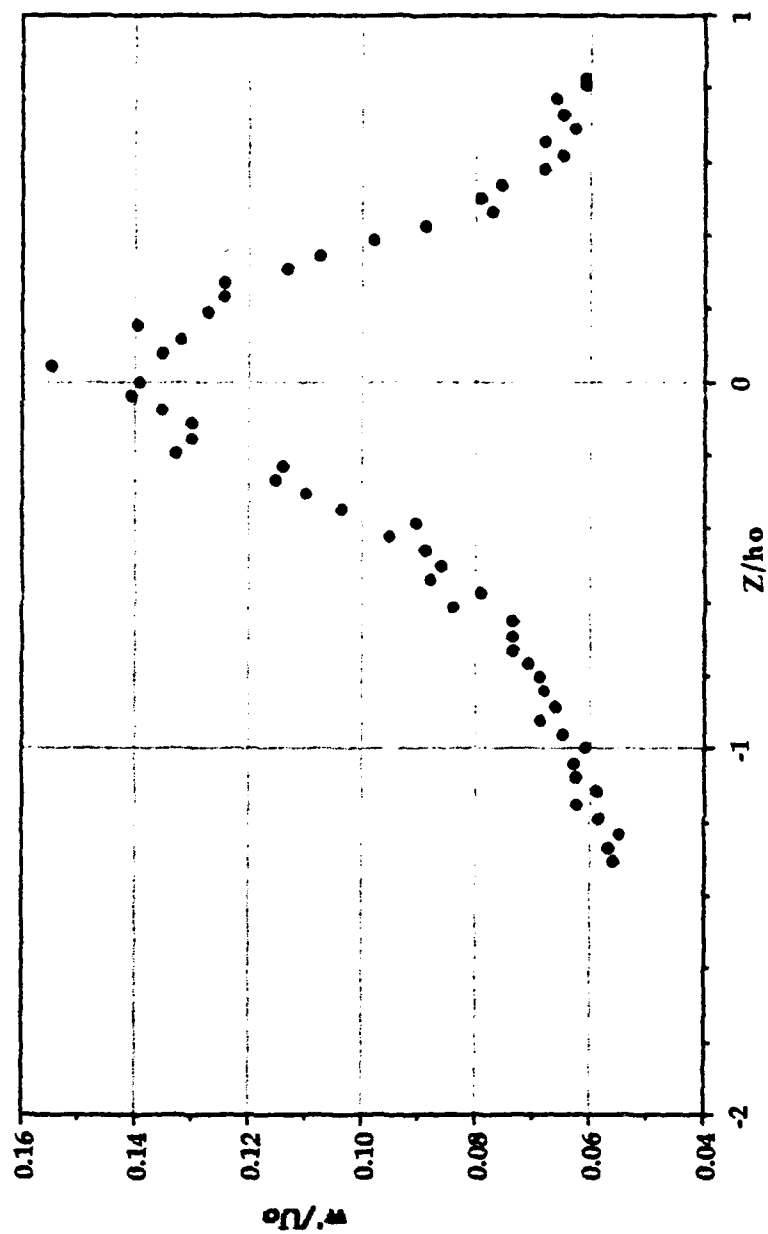


Figure 28. w'/U_0 versus Vertical Distance for $Y/h_0 = -0.40$ and $x/c = 5.02$

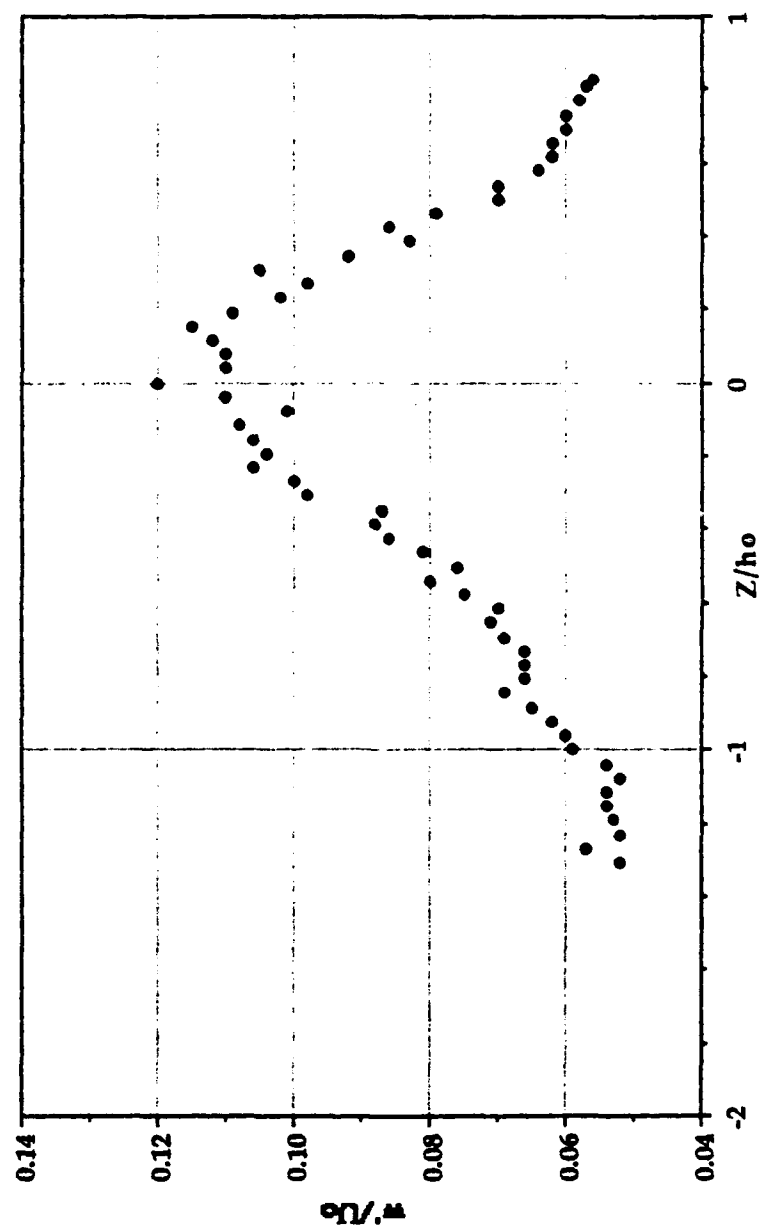


Figure 29. w'/U_0 versus Vertical Distance for $Y/h_0 = -0.15$ and $x/c = 5.02$

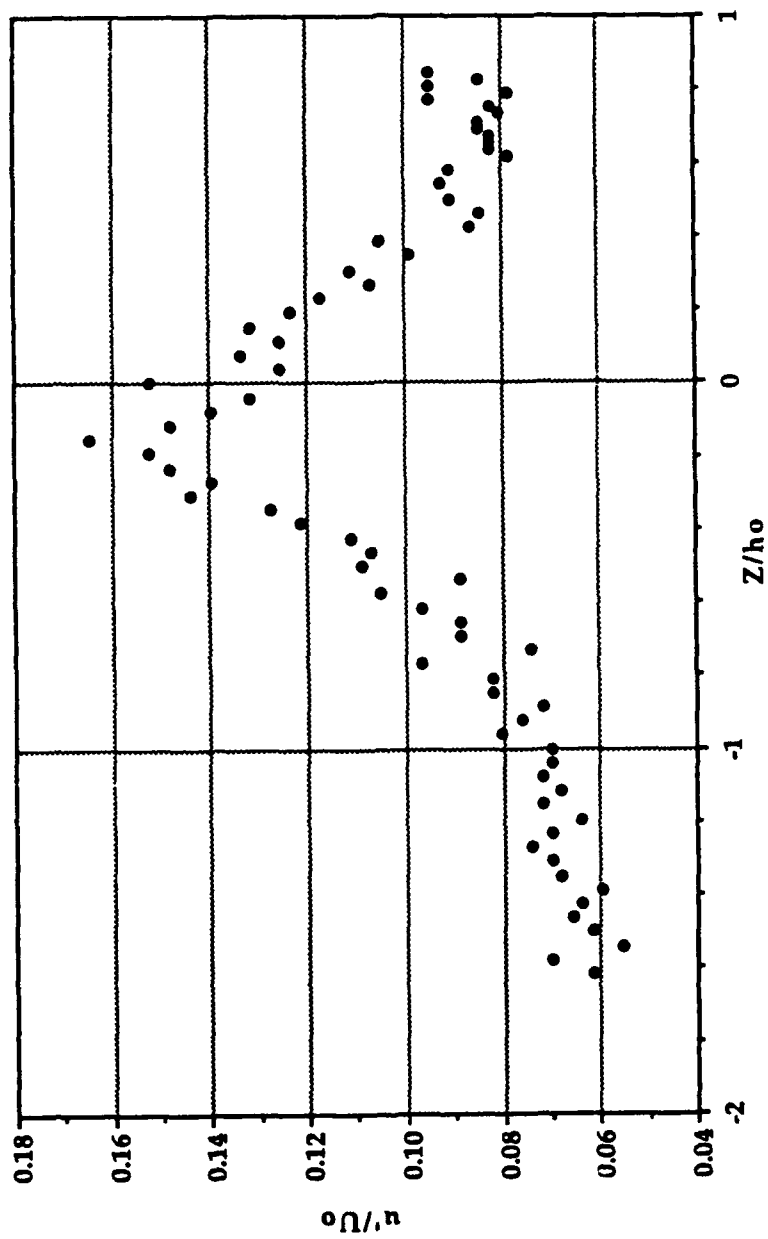


Figure 30. u'/U_0 versus Vertical Distance for $Y/h_0 = -0.46$ and $x/c = 6.52$

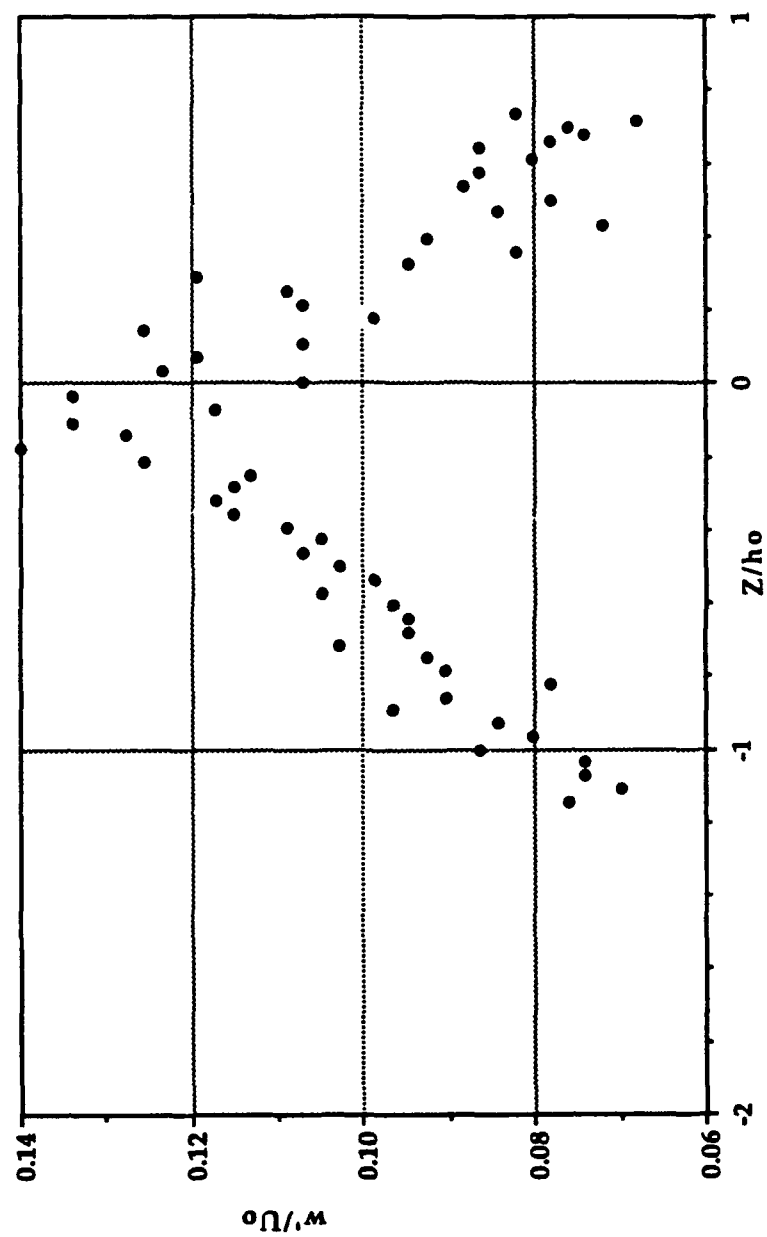


Figure 31. w'/U_0 versus Vertical Distance for $Y/h_0 = -0.25$ and $x/c = 6.52$

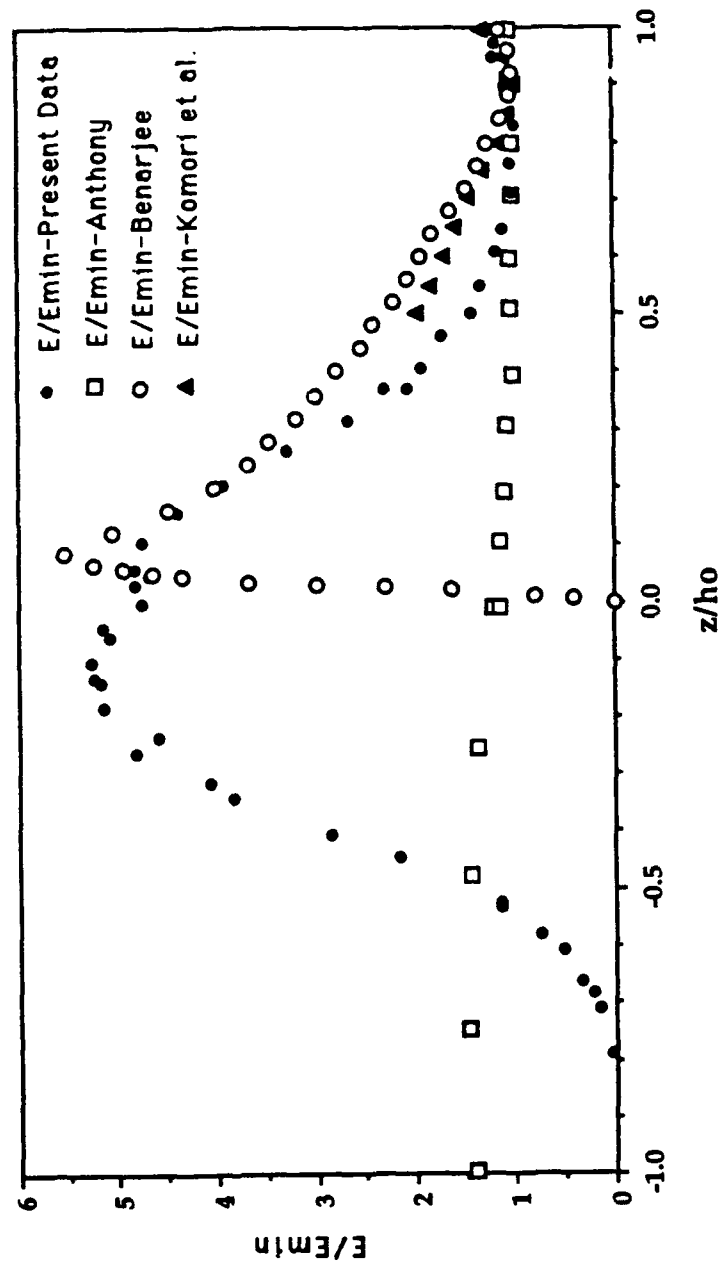


Figure 32. Normalized Turbulent Kinetic Energy versus Vertical Distance

REFERENCES

1. Anthony, D. G., 1990, "The Influence of a Free Surface on the Development of Turbulence in a Submerged Jet with a Clean or Contaminated Free Surface", Ph. D. thesis, University of Michigan.
2. Anthony, D. G. and Willmarth, W. W., 1992, "Turbulence Measurements in a Round Jet beneath a Free Surface", *Journal of Fluid Mechanics*, Vol. 243, Oct. , pp. 699-720.
3. Brumley, B., 1984, "Turbulence Measurements near the Free Surface in Stirred Grid Experiments", *Gas Transfer at Water Surfaces* (eds. W. Brutsaert and H. Jirka), Reidel-Dordrecht, The Netherlands, pp. 83-86.
4. Dickey, T. D., Hartman, B., Hammond, D., and Hurst, E., 1984, "A Laboratory Technique for Investigating the Relationship between Gas Transfer and Fluid Turbulence", *Gas Transfer at Water Surfaces* (eds. W. Brutsaert and H. Jirka), Reidel-Dordrecht, The Netherlands, pp. 93-100.
5. Durand, W. F. (ed.), 1963, *Aerodynamic Theory*, Vol. III, pp. 280-306. Dover.
6. Harvey, J. K. and Perry, F. J., 1971, "Flow Field Produced by Trailing Vortices in the Vicinity of the Ground", *AIAA Journal*, Vol. 9, No. 12, pp. 1659-1660.
7. Hunt, J. C. R. and Graham, J. M. R., 1978, "Free-Stream Turbulence Near Plane Boundaries", *Journal of Fluid Mechanics*, Vol. 84, Jan., pp. 209-235.
8. Jacquin, L., Leuchter, O., and Geffroy, P., 1989, "Experimental Study of Homogeneous Turbulence in the Presence of Rotation", *Turbulent Shear Flows 6* (eds. J. C. André et al.), pp. 46-57, Springer-Verlag.
9. Komori, S., Nagaosa, R., Murakami, Y., Chiba, S., Ishii, K., and Kuwahara, K., 1993, "Direct Numerical Simulation of Three-Dimensional Open-Channel Flow with Zero-Shear Gas-Liquid Interface", *Physics of Fluids A*, Vol. 5, No. 1, pp. 115-125.
10. Komori, S., Ueda, H., Ogino, F., and Mizushima, T., 1982, "Turbulence Structure and Transport Mechanism at the Free Surface in an Open Channel Flow", *International Journal of Heat and Mass Transfer*, Vol. 25, No. 4, pp. 513-521.
11. Lam, K. and Banerjee, S., 1992, "On the Condition of Streak Formation in a Bounded Turbulent Flow", *Physics of Fluids A*, Vol. 4, No. 2, pp. 306-320.

12. Loewen, S., Ahlborn, B., and Filuk, A. B., 1986, "Statistics of Surface Flow Structures on Decaying Grid Turbulence", *Physics of Fluids*, Vol. 29, No. 8, pp. 2388-2397.
13. Neubert, D. E., Jr., 1992, *Trailing Vortex/Free-Surface Interaction*, M.S. Thesis, Naval Postgraduate School, Monterey, California.
14. Rashidi, M. and Banerjee, S., 1988, "Turbulence Structure in Free Surface Channel Flows", *Physics of Fluids*, Vol. 31, No. 9, pp. 2491-2503.
15. Shabaka, I. M. M., Mehta, R. D., and Bradshaw, P., 1985, "Longitudinal Vortices Imbedded in Turbulent Boundary Layers. Part 1. Single Vortex", *Journal of Fluid Mechanics*, Vol. 155, pp. 37-57.
16. Sarpkaya, T., 1986, "Trailing-Vortex Wakes on the Free Surface", *Proceedings of the 16th Symposium on Naval Hydrodynamics*, National Academy Press, Washington, D. C., pp. 38-50.
17. Sarpkaya, T., 1989, "Computational Methods with Vortices—1988 Freeman Scholar Lecture", *Journal of Fluids Engineering, Transactions of ASME*, Vol. 111, No. 1, pp. 5-52.
18. Sarpkaya, T., 1992a, "Three-Dimensional Interactions of Vortices with a Free Surface", AIAA Paper No. 92-0059.
19. Sarpkaya, T., 1992b, "Interaction of a Turbulent Vortex with a Free Surface", *Proceedings of the Nineteenth Symposium on Naval Hydrodynamics*, National Academy Press, Washington, D. C., (in press).
20. Sarpkaya, T., Elnitsky, J., and Leeker, R. E., 1988, "Wake of a Vortex Pair on the Free Surface", *Proceedings of the 17th Symposium on Naval Hydrodynamics*, National Academy Press, Washington, D. C., pp. 47-54.
21. Sarpkaya, T. and Neubert, D. E., Jr., 1993, "Interaction of a Streamwise Vortex with a Free Surface," AIAA Paper No. 93-0556.
22. Sarpkaya, T. and Suthon, P. B. R., 1991, "Interaction of a vortex couple with a free surface", *Experiments in Fluids*, Vol. 11, pp. 205-217.

INITIAL DISTRIBUTION LIST

	<u>No. Copies</u>
1. Defense Technical Information Center Cameron Station Alexandria, VA 22304-6145	2
2. Librarian, Code 52 Naval Postgraduate School 411 Dyer Rd., Rm. 104 Monterey, CA 93943-5101	2
3. Department Chairman Mechanical Engineering Department, Code ME Naval Postgraduate School 699 Dyer Rd, Rm. M3 Monterey, CA 93943-5108	1
4. Professor T. Sarpkaya Mechanical Engineering Department, Code ME-SL Naval Postgraduate School 699 Dyer Rd, Rm. M2 Monterey, CA 93943-5108	5
5. Naval Engineering Curricular Office Code 34 Naval Postgraduate School 699 Dyer Rd, Rm. 220 Monterey, CA 93943-5109	1
6. LT John B. Carroll, USN C/O Mrs. K. Snyder 7916 Peyton Forest Trail Annandale, VA 22003-5000	2